2012

TEMPERATURE AND STRAIN CONTROLLED OPTIMIZATION OF STABILIZATION OF POLYACRYLONITRILE PRECURSOR FIBERS

Mark Parr Taylor
University of Kentucky, markparrtaylor@gmail.com

STUDENT AGREEMENT:

I represent that my thesis or dissertation and abstract are my original work. Proper attribution has been given to all outside sources. I understand that I am solely responsible for obtaining any needed copyright permissions. I have obtained and attached hereto needed written permission statements(s) from the owner(s) of each third-party copyrighted matter to be included in my work, allowing electronic distribution (if such use is not permitted by the fair use doctrine).

I hereby grant to The University of Kentucky and its agents the non-exclusive license to archive and make accessible my work in whole or in part in all forms of media, now or hereafter known. I agree that the document mentioned above may be made available immediately for worldwide access unless a preapproved embargo applies.

I retain all other ownership rights to the copyright of my work. I also retain the right to use in future works (such as articles or books) all or part of my work. I understand that I am free to register the copyright to my work.

REVIEW, APPROVAL AND ACCEPTANCE

The document mentioned above has been reviewed and accepted by the student's advisor, on behalf of the advisory committee, and by the Director of Graduate Studies (DGS), on behalf of the program; we verify that this is the final, approved version of the student's dissertation including all changes required by the advisory committee. The undersigned agree to abide by the statements above.

Mark Parr Taylor, Student

Dr. Rodney Andrews, Major Professor

Dr. James M. McDonough, Director of Graduate Studies

TEMPERATURE AND STRAIN CONTROLLED OPTIMIZATION OF STABILIZATION OF POLYACRYLONITRILE PRECURSOR FIBERS

THESIS

A thesis submitted in partial fulfillment of the
requirements for the degree of Master of Science in
Mechanical Engineering in the College of Engineering
at the University of Kentucky

By

Mark Parr Taylor

Lexington, KY

Director: Dr. Rodney Andrews, Professor of Chemical and Materials Engineering

Lexington, KY

2012

ABSTRACT OF THESIS

TEMPERATURE AND STRAIN CONTROLLED OPTIMIZATION OF STABILIZATION OF POLYACRYLONITRILE PRECURSOR FIBERS

Carbon fiber is one of the leading materials for high strength and modulus, and light weight applications. Improvements in carbon fiber properties are directly dependent on all aspects of manufacture, especially the process of stabilization. Therefore, it is the goal of this thesis to study the effects of the temperature and strain profile of the stabilization process, and the resulting carbon fiber tensile properties. In addition, the precursor fibers used were spun under two different draw ratios, to study the effects of the spinning parameters. Results indicated through DMA studies that completeness of stabilization reactions can be gauged by the peak and leveling of induced stress while fibers are stabilized in isostrain conditions. Through this method, carbon fiber tensile properties were maintained from the prior methods, but saved significant time for processing. Stress vs. strain tests throughout the stabilization process created a baseline for understanding the maximum capable strain on fibers throughout the stabilization process. Lastly, this information was summarized, combined, and basic mechanical engineering principles discussed for a continuous stabilization furnace with strain control, so that further research into the stabilization process can incorporate carbon fibers made with *in situ* stretch control.

KEYWORDS: Carbon Materials, Carbon Fiber, Stabilization, Polyacrylonitrile, Optimization

Mark Parr Taylor

27 April 2012

TEMPERATURE AND STRAIN CONTROLLED OPTIMIZATION OF STABILIZATION OF POLYACRYLONITRILE PRECURSOR FIBERS

By

Mark Parr Taylor

Rodney J. Andrews, Ph.D.
Director of Thesis

James M. McDonough, Ph.D.
Director of Graduate Studies

27 April 2012

Dedicated to Angela

ACKNOWLEDGEMENTS

I would like to thank my advisor, Dr. Rodney Andrews, for his encouragement and council throughout this project. Without his questions, advice, and perspective, this thesis would not have been possible. I also want to thank Dr. Mark Meier and Dr. Tingwen Wu for serving on my examining committee. I am grateful for their support throughout my academic and research career, and in their time devoted to this project.

A special thanks goes to Dr. Matthew Weisenberger, as the inspiration for me to research such an exciting and complex research subject, and as my closest mentor throughout this thesis. Without his support and knowledge, I have no doubt that this thesis would not have been completed.

I would also like to extend thanks to my colleagues in the Carbon Group, and the Center for Applied Energy Research as a whole. Ashley Morris, David Jacques, John Craddock, Terry Rantell, Dali Qian, Roger Perrone, Keith Etheredge, among others have had a supporting hand in making this project a reality.

Lastly, I would like to thank my loving girlfriend Angela. She is the primary driving force for me to be the best I can be, and has been a constant source of encouragement and support. I would also like to thank my parents, siblings, and friends for being so supportive, especially during my graduate school tenure.

TABLE OF CONTENTS

LIST OF TABLES

LIST OF FIGURES

DISCLAIMER

The student was instructed by his committee, due to a variety of concerns, to remove certain details and results from this work pertaining to process parameters before publishing online.

1 INTRODUCTION

1.1 Motivation

Carbon fiber is a unique material that possesses high tensile strength, modulus, and low weight. Throughout decades of research since the mid 20th century, carbon fibers based on polyacrylonitrile (PAN) precursor fibers have pulled ahead of other materials such as rayon and pitch based carbon fibers, for their desirable tensile properties, fewer defects, higher carbon yield, and toughness. Research and industry have been continuously improving the properties and manufacturability of carbon fibers, and in doing so, the level of demand for the material is ever-growing as uses and applications are expanded. In aerospace, wind energy, sporting goods, and high performance vehicles, carbon fiber and carbon fiber composites are replacing plastics, metals, and woods as a superior structural material.

The manufacture of PAN-based carbon fibers takes place in three main steps. The first is the spinning and drawing of the polymer solution to create precursor fibers. The second is to stabilize those fibers under low heat treatment (< 300 °C) to alter the fibers molecularly into a robust ladder structure and introduce stronger bonds in the polymer chains. The final step is to carbonize the fibers, removing the non-carbon atoms creating carbon fiber with the desired properties. Each step is paramount to the fibers achieving optimum properties, and continued research brings carbon fiber closer to achieving the theoretical tensile properties that make it such a promising material.

Extensive research has been performed to optimize the properties of carbon fiber, but each of the three steps of carbon fiber manufacture possesses dozens, if not hundreds, of independent variables that affect the final product. Stabilization is regarded as one of the most complex and crucial processes of carbon fiber manufacture, as it bridges the gap between spinning and carbonization. The parameters necessary for an optimized stabilization procedure are dependent on the quality of the spun precursor fibers, and ultimately affect the properties seen after carbonization. In this work, it is the goal to

take a given precursor fiber, and analyze the temperature and stretching profile that makes up the process of stabilization. With this understanding, the objective will be to create a carbon fiber with better tensile properties and also to improve the manufacturability by investigating optimized procedures for stabilization.

1.2 Introduction and Outline

The objective of this project was to produce an optimized stabilization profile for a given set of polyacrylonitrile precursor fibers. PAN fibers were made from an 18 wt% homopolymer PAN dope (ir solution in N,N-dimethylacetamide (DMAc)), wet spun under two different draw ratios: 5.9 and 10.7, resulting in precursor fibers of 24.2 and 20.6 microns in (equivalent circular) diameter, respectively.

Chapter 3 begins analysis of the precursor fibers through use of differential scanning calorimetry (DSC). Linear temperature ramps ranging from 1.0 to 20.0 °C/min were used in order to find the activation energies of the precursor fibers of both draw ratios, using the methods outlined by Kissinger and Ozawa. The temperature ramps were also used to study the onset points to the reactions of stabilization, which were necessary for developing a starting point for development of an optimized stabilization temperature profile.

Chapter 4 continues to analyze the temperature profile for optimized stabilization. Experiments with dynamic mechanical analysis (DMA) observed the situ stress accumulated in the fibers during stabilization while maintaining isostrain conditions. This method was used to find the relationship between a matrix of temperature parameters and the resulting stress profile. The main points of observation were the maximum slopes of the stress (with respect to time), the maximum stresses, and the corresponding times associated with those values. Taking a selection of fibers for batch processing, fibers were stabilized under some of the studied profiles, then carbonized and tested under identical conditions. The relationship between the stabilization parameters, the stress during stabilization, and the final carbon fiber properties was then made.

Chapter 5 makes a foundation for continued research in stretching fibers during stabilization. Stress vs. strain tests were performed on fibers in the process of stabilization, by holding them in isostrain in the DMA, proceeding with a temperature profile, and interrupting the heat treatment for the test to failure. This was to find the region during the temperature profile that was best for stretching, and to observe the maximum amount of stretching capable throughout stabilization. Additionally, an array of stain rate tests were performed in order to observe any effects of strain rate on the maximum amount of strain until fiber breakage.

Lastly, Chapter 6 will provide an overview of the stabilization furnace built for pitch fibers, and the efforts to make it capable to stabilize PAN based precursor fibers. Considerations for stretching zones and roller placement were made based on the research and experimentation of when stretching should occur and the ideal temperature profile for stabilization. The constraints and limitations of the furnace were also analyzed. A program was then built based on the findings for the optimized stabilization procedure, with inputs that can accommodate different precursors, giving it the flexibility to be used in the future under a large variety of different parameters.

2 REVIEW OF LITERATURE

2.1 Introduction

Carbon fiber is a unique engineering material that has seen significant growth in research and use since the mid-twentieth century with R.C. Houtz observing the color change of stabilizing Orlon (a DuPont PAN fiber) in 1950 and Union Carbide in 1959 creating carbon products with the aim of high strength[1]. Carbon fibers have been applied in aircraft, automobiles, space applications, super conductors, and in the biomedical field[2-4]. Throughout the years carbon fiber has seen improved properties and manufacturability, and as a result, has grown as an industry. Carbon fiber is made in three general steps: Spinning of the precursor fibers, stabilization of the precursor fibers to prepare for the final stage, carbonization (and potentially graphitization). Much research has been done to connect the dots among these complex processes. It can be observed that the process to manufacture optimized carbon fiber is highly dependent on the path that led to the step currently under study. In this literature review, the goal is to create a general understanding of the links between the process of stabilization and the ultimate carbon fiber properties. It cannot, however, be avoided to mention the "path-dependent" repercussions that spinning has on stabilization, and how the former two processes affect carbonization/graphitization.

2.2 Carbon Fiber

2.2.1 Introduction

Carbon fiber has the desirable traits of having very high strength and modulus, yet low density and coefficient of thermal expansion. Combine those traits with the ability to weave the fibers into a fabric or prepreg that can take nearly any shape in a composite materials form, and it is not difficult to understand why a growing demand exists for the material.

2.2.2 Carbon Fiber Properties

Carbon fibers are a desirable material for its light weight, high strength and modulus, and versatility. Being a fairly modern material, carbon fiber has seen significant advancement in recent decades. Advances in all aspects of carbon fiber production:

spinning, stabilization, and carbonization/graphitization have been made. Stabilization is regarded by many to be the most significant area in carbon fiber manufacture where the properties can be advanced further. [5]

To quickly summarize the progress made in manufacturing carbon fiber with desirable properties, initial fibers produced were not strong by today's standards until 1970 when tension control and stretching was implemented in the stabilization process [6]. Shortly thereafter, Toray Industries was producing commercial fibers, T300, with a tensile strength of 3.5 GPa. And later, the T1000 fibers achieved 7.06 GPa tensile strength. PAN-based fiberes with a Young's modulus as high as 490 GPa were also achieved. Many research teams have studied carbon fiber manufacture, and have concentrated on tension control during stabilization[7-13]. With those efforts carbon fiber properties have advanced and will continue to develop.

2.2.3 Carbon Fiber Production

PAN fibers are established as the primary precursor used in commercial carbon fiber production [4, 14-16]. Most PAN fibers ultimately have gone to use in the area of composites [17], initially used in military and space applications, their high end properties have been ideal for expansion into the automotive and commercial aerospace industries[18]. The production of PAN based carbon fiber has grown significantly: from 19 million lbs per year in 1989 [19] to nearly 72 million lbs per year in 2005[20].

2.3 Precursor Fiber Structure and Chemistry

2.3.1 Introduction

Precursor fibers can be produced from an array of materials, but for commercial scale production the primary choices are polyacrylonitrile (PAN), pitch, and rayon[2, 4, 21]. Of those three, PAN fibers have stepped ahead as the precursor of choice, as rayon has a low carbon yield [4, 22-26] and pitch based fibers tend to have lower toughness, may have more voids within the fiber, and are generally more expensive[5, 27]. For this paper, precursor fibers made of polyacrylonitrile (homopolymer) will be discussed.

During stabilization, precursor fibers undergo physical and chemical changes. In order to recognize the reactions that take place, it is important to have a firm understanding of the structure of the precursor fiber before stabilization.

2.3.2 Precursor Fiber Molecular Structure affecting Stabilization

Polyacrylonitrile precursor fibers have a molecular structure that is relatively insoluble with a high melting point[28]. It is a chain of carbon with nitrile groups throughout, as seen in the figure below.

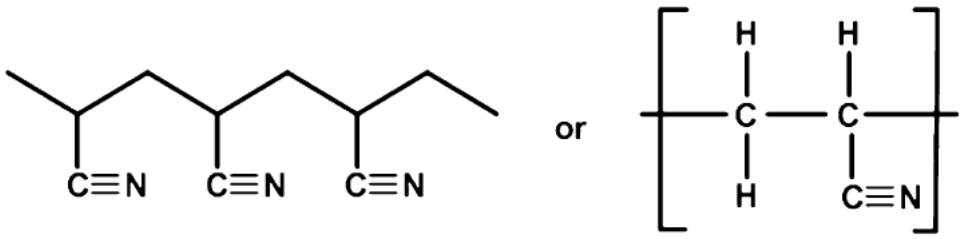

Figure 2-1: Molecular structure of polyacrylonitrile [29][1]

Oligomerization of the nitrile groups occurs in three steps, initiation, propagation, and termination. Depending on the precursor fiber chemistry, initiation can start by one of two mechanisms: free radical initiation or an ionic mechanism[5]. When the precursor is a homopolymer (such as the fibers in this work), free radical mechanisms are the initiator. Free radicals are made from the breaking of C ≡ N bonds that initiate the cyclization process, and the initiation is what becomes the rate determining factor in cyclization[30]. When initiated by free radicals, propagation is quite rapid, which results in a strong exothermic reaction that may lead to damage, fusion, or melting of the fibers if not properly controlled.

Regarding the other means of initiation, ionic mechanisms are present when comonomers are added to the polyacrylonitrile. In this case, cyclization is initiated by the fission of the ionic groups[5]. Initiation by this method is preferred as the reactions are less sudden

[1] Reprinted from *Polymer Degradation and Stability*, 92, Rahaman, M.S.A; Ismail, A.F.; Mustafa, A., "A Review of Heat Treatment on Polyacrylonitrile Fiber," Pg 1421-1432, 2007, with permission from Elsevier

and produce a reduced exothermic reaction over a broader temperature range (lowering the initiation temperature)[31-39]. Comonomers have also been found to improve the mobility of the chains of polymer, which can improve the spinning process as well[37, 39]. Comonomers that are common in research and industry include vinyl acids, esters, amides, and salts of vinyl compounds, with particular interest directed on acid and ester comonomers. To demonstrate, for example, the initiation of acid comonomers, such as acrylic acic (AA), methacrylic acid (MA), and itaconic acid (IA), the following reaction mechanism has been shown:

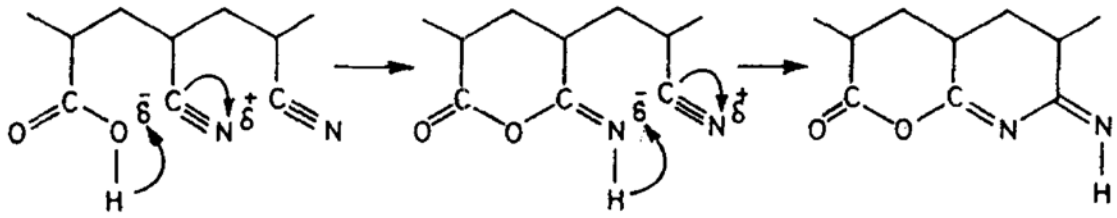

Figure 2-2: Cyclization involving reaction mechanism of acidic comonomers[5][2]

Following initiation and propagation, is termination. Termination of local reactions occurs when a nitrile group fails to propagate. This has been attributed to several reasons, including the addition of a hydrogen free radical to the nitrile groups leading to ammonia formation, combination of two growing chains, steric hindrance, or lack of availability of free nitrile groups[36].

2.3.3 Precursor Fiber Macro-Molecular Structure affecting Stabilization

The macro-molecular structure of polyacrylonitrile precursor fibers can best be described as a part of one of two categories, amorphous or quasi-crystalline. The quasi-crystalline region consists of the carbon backbone with nitrile groups forming an irregular helical pattern. In between those regions are volumes that are amorphous, or disordered, regions. These volumes are made up of chain ends, defects, entanglements, and

[2] Reprinted from *Journal of Macromolecular Science*, 37, "Thermal Stabilization of Acrylic Precursors for the Production of Carbon Fibers: An Overview," Bajaj, P.; Roopanwala, A.K., 1997 with permission from Taylor and Francis www.tandfonline.com

comonomer sequences [40]. A proposed morphological model by Warner [7] of PAN fiber showing those ordered and disordered regions can be seen below.

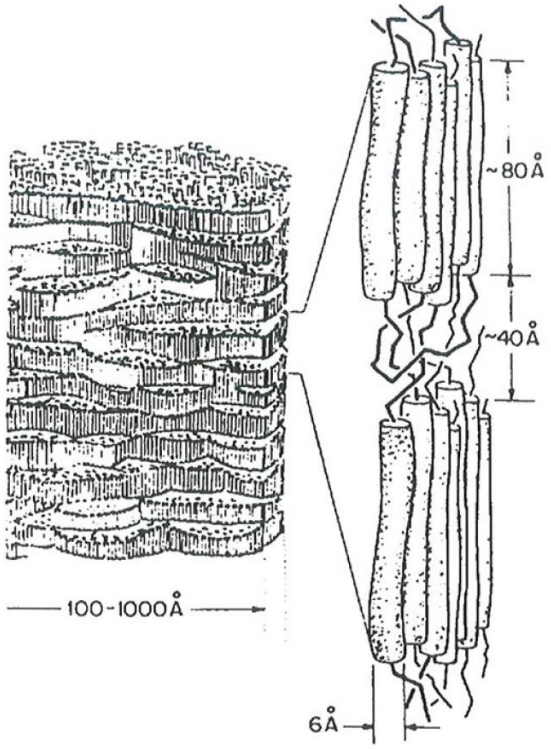

Figure 2-3: Morphological model of PAN fiber proposed by Warner[41][3]

Looking closer into the irregular helical structure of the PAN molecules in the quasi-crystalline region, a proposed structure was put forward by Olive[39].

[3] With kind permission from Springer Science + Business Media: *Journal of Materials Science and Engineering*, Oxidative Stabilization of Acrylic Fibres, 14, 1979, 1893-1900, Warner, S.B., Uhlmann, D.R., Fig. 5

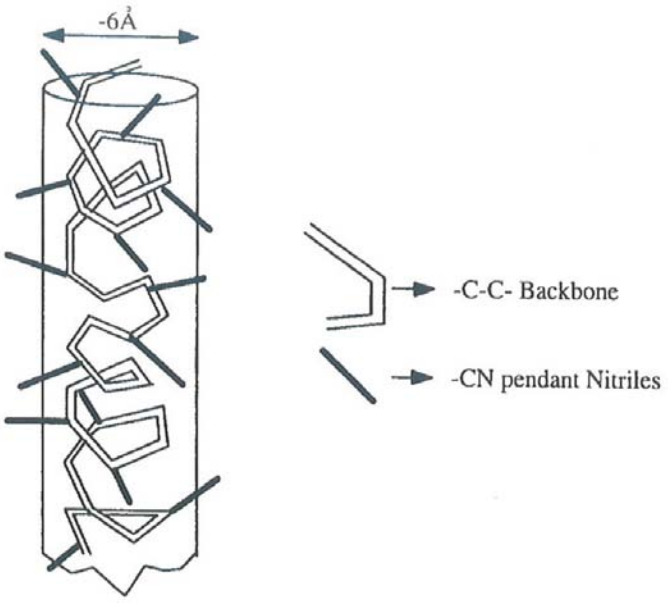

Figure 2-4: Proposed irregular helical structure of PAN by Olive [7][4]

In a study comparing two precursor fibers under equivalent stabilization conditions, precursor fibers made with lower amounts of comonomers resulted in higher crystallinity in the stabilized fibers, whereas those with higher comonomer concentrations had reduced crystallinity and higher oxygen content. This follows previous research, where it has been shown that one of the main drivers for cyclization initiation is from the amorphous regions of the fiber, which in turn can be created by comonomers [7, 42, 43].

Additionally, precursor fibers with higher concentrations of quasi-crystalline regions maintain higher stress during stabilization[12]. This must be kept in mind when planning the stretching ratios during stabilization. The same stretch profile between fibers of differing crystalline structures will see that the more ordered fiber will not stretch as much, or if forced to stretch as much, will see damage to the fiber. This is because the amorphous regions of fibers are more amenable to rearranging their molecules and stretching[44]. To summarize the last two points, higher comonomer concentrations (among other things) result in precursor fibers with more amorphous regions, which

[4] With kind permission from Springer Science + Business Media: *Advances in Polymer Science* "Molecular Interactions and Macroscopic Properties of Polyacrylonitrile and Modal Substances," 1979, Henrici-Olive, G.; Olive, Salvador, Fig. 1.

results in fibers that are more compliant in stabilization stretching (in addition to aiding in the initiation of stabilization reactions).

2.3.4 Precursor Fiber Qualities affecting Stabilization

Spinning conditions pose a significant correlation to the quality of the precursor fiber, stabilization parameters, and ultimate carbon fiber tensile properties. Without quality precursor fiber, the best stabilization procedures are limited in their ability to produce quality carbon fiber. This creates the necessity to understand what makes desirable precursor fibers, and why good precursor fibers result in better stabilization. This subject has been extensively researched as much, if not more, than the effects of stabilization on carbon fiber properties, and only a general knowledge will be provided here.

Acrylic fibers are made from either wet, dry, or dry-jet-wet spinning techniques. Wet spinning accounts for approximately 85% of acrylic fiber production[45], and is the method used in this project. However, dry-jet-wet spinning has been found to improve the precursor fiber qualities by increasing total draw ratio, improving the molecular alignment along the fiber axis, and producing a fine linear density[46].

As a general rule, the smaller the diameter of the precursor fiber, the easier for energy (heat) and mass diffusion for stabilization. Fibers of 10-12 microns have been known to be more compatible with stabilization, as the increased surface area to volume ratio improves heat dissipation, and encourages thorough and uniform gas diffusion [47, 48]. The more uniform diffusion will help prevent the formation of a skin-core structure seen in larger diameter fibers. In addition, they generally have less defects from spinning.

Post-spinning modifications, including stretching at elevated temperatures in air, nitrogen, or even a fluid such as glycerol, generally shows improvement in the resultant carbon fibers[49]. Stretching at elevated temperatures is done above the glass transition temperature, where the fibers are more fluid and compliant. Stretching has been shown to improve the molecular orientation along the fiber axis, lowering the activation energy and temperature of initiation for the cyclization reactions, and ultimately leading to strong carbon fibers[50].

2.4 Precursor Stabilization Reactions

2.4.1 Introduction

Thermo-oxidative stabilization of polyacrylonitrile refers to the low temperature (generally 200-350 °C) conversion of the polymer fibers to a high temperature resilient fiber through the means of chemical reactions. The conversion is necessary for the fibers to survive carbonization and graphitization with the highest possible carbon yield and superior properties. The major chemical reactions are oxidation, dehydrogenation, cyclization, and cross-linking. After such reactions have occurred, the molecular structure will form a thermally stable ladder structure (which can be described as a linear chain of fused pyridine rings) with oxygen-containing groups facilitating inter-molecular linkages[51].

2.4.2 Oxidation

Oxidation occurs when the polyacrylonitrile precursor fiber takes in oxygen during stabilization. The oxidizing environment primarily used in stabilization is air. Oxidation is necessary for dehydrogenation.

Fitzer and Muller proposed that oxygen atoms can bond to PAN molecules in numerous ways [38]. They found that when stabilized in oxygenated versus inert atmospheres, PAN had a higher activation energy and frequency factor when stabilized in the former. This showed that oxygen can be an initiator for the formation of the activated center for cyclization. Not all oxygen entering the polymer is used for dyhydrogenation, as a result, several ideas to explain the presence of oxygen after cyclization have been proposed. Possible structures include the bridging of ether links, carbonyl groups, donation of lone pair electrons, and the formation of hydroxyl and carbonyl groups[52, 53]. Accounts for general guidelines for the steady-state uptake of oxygen vary, from around 8 wt% cited by Fitzer[54] to approaching 14 wt% by Watt[1].

2.4.3 Dehydrogenation

Dehydrogenation is the process where hydrogen leaves the fiber, typically with oxygen as water, and a double bond results between two carbons, stabilizing the carbon chain. The double bond formed in the reaction results in better thermal stability and reduces chain

scission during the high temperatures endured during carbonization[53]. Occurring in two steps, dehydrogenation starts with oxidation and ends with the elimination of water. Therefore, it is desirable to stabilize the fiber in an atmosphere with oxygen present, which is usually air. Additionally, this shows that the process of dehydrogenation is primarily a function of oxygen diffusion, where the process can be controlled with variables including oxygen concentration at the source, surface to volume ratio of the polymer, and boundary layer conditions (e.g. ambient, turbulent air mixing).

In 1975, Fitzer et al conducted a series of stabilization experiments with Differential Thermal Analysis (DTA) and control of the air/nitrogen environment[38]. Their findings demonstrated that the reaction of dehydrogenation can occur either before or after cyclization, as seen in the Figure 2-6.

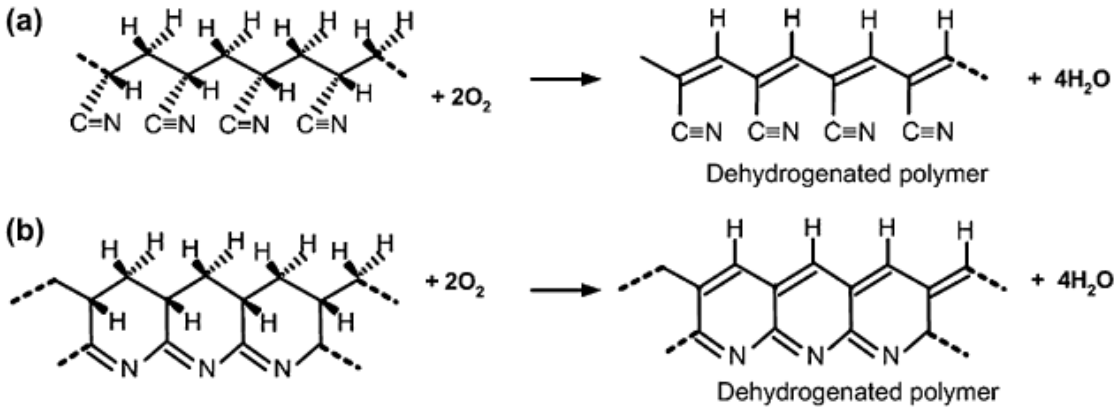

Figure 2-5: Dehydrogenation can take place either (a) before or (b) after cyclization of the PAN polymer [29][5]

But even in the findings just mentioned, dehydrogenation is a relatively slower process in stabilization, and it prefers to occur on already cyclized chains. Through research comparing the results of DSC and FTIR, Liu et al found that dehydrogenation occurs close to simultaneously with oxidation[55]. In a study to find the activation energies and frequency factors of the individual reactions, the fibers were stabilized in an inert atmosphere, where the reactions of cyclization would occur independently, and in a

[5] Reprinted from *Polymer Degradation and Stability*, 92, Rahaman, M.S.A; Ismail, A.F.; Mustafa, A., "A Review of Heat Treatment on Polyacrylonitrile Fiber," Pg 1421-1432, 2007, with permission from Elsevier

relatively short and intense manner. Those cyclized fibers were stabilized again in air, where it was found that oxidation and dehydrogenation require a significantly lower activation energy, and will occur over a broader length of time relative to the reactions of cyclization[55]. These findings suggest (at least for the ~9.5-11 micron diameter homopolymer PAN precursor used) that dehydrogenation is the limiting factor when attempting to fully stabilize fiber.

2.4.4 Cyclization

Cyclization is the most important reaction during stabilization. It takes place when the nitrile bond (C≡N) reacts to form a double bond, and a fused pyridine ring chain structure is formed. This structure is far more thermally stable than the former nitrile bond. Unlike dehydrogenation, cyclization does not need the presence of oxygen to take place, so it can occur in an inert atmosphere. This trait is widely used to separate cyclization from the other stabilization reactions in thermal analysis. Additionally, this is a result of cyclization being an energy dependent reaction, as opposed to mass dependent; therefore, the reaction is controlled with temperature and time parameters to ensure energy (heat) diffusion into the polymer. The molecular structure of the PAN precursor as it undergoes the above mentioned reactions can be summarized below.

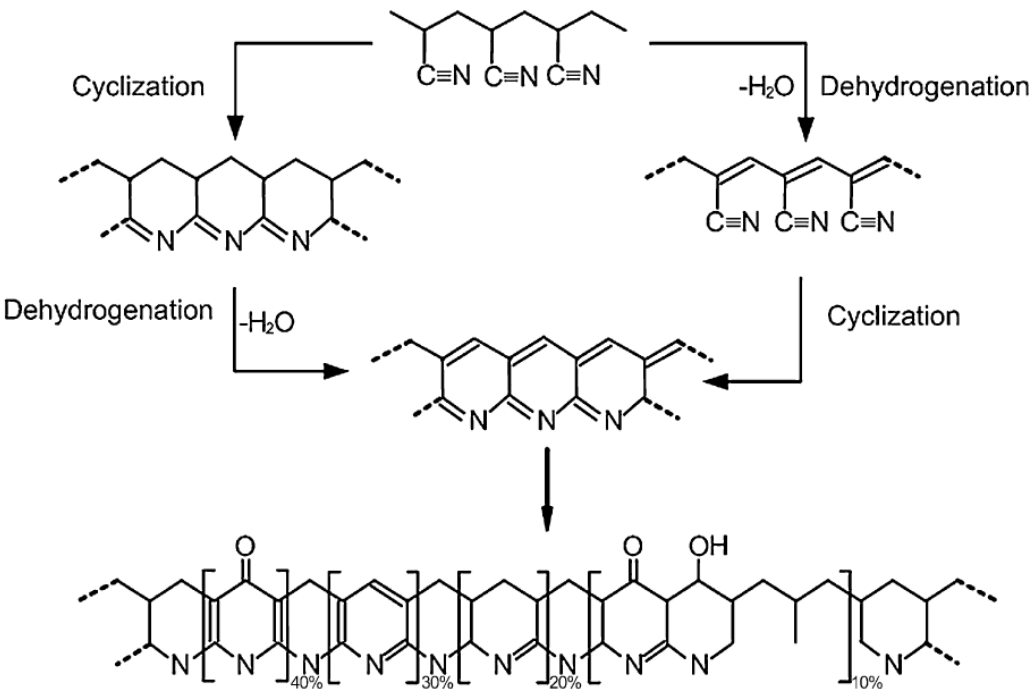

Figure 2-6: Proposed structure of PAN molecules during stabilization [2, 18, 56][6]

Cyclization is the reason why stabilized fibers change color from white to yellow to brown to black[57-59]. An old and quick test to see if fibers have been thoroughly stabilized is to place them under a flame. If they glow and do not burn, that is indicative that the fibers have gone through cyclization[57].

The initiation of cyclization has been linked to several sources. It could start at impurities in the polymer, such as catalyst fragments, residual polymerization products, or inhibitors[60]. It can also be initiated in chain end groups [61], random initiation of hydrogen atoms to the nitrile[62], or the nitrile transforming to an axomethine[63]. Friedlander suggested that cyclization was initiated by the presence of a ketonnitrile by hydrolysis during polymerization[58], and Peebles et al proposed that it could be because of hydrolysis of nitriles to acids during polymerization[64].

[6] Reprinted from *Carbon* 27-5, Fitzer, E., "PAN-Based Carbon Fibers- Present State and Trend of the Technology from the Viewpoint of Possibilities and Limits to Influence and to Control the Fiber Properties by the Process Parameters," Pg 621-645, 1989, with permission from Elsevier.

Cyclization is an exothermic reaction, and it has the potential to damage the fibers if done in too short a duration[65]. The fibers can shrink excessively, lose significant mass, and even melt and fuse together. Conversely, if the stabilization procedure is too conservative and the fibers are only partially stabilized, unstabilized portions will volatize during carbonization and graphitization, significantly weakening the end product.

2.5 Stabilization Factors that affect Carbon Fiber Quality: Time and Temperature

2.5.1 Introduction

As mentioned before, cyclization is an exothermic reaction. When stabilization is performed too quickly, the fibers can become damaged and when done too conservatively (lower max temperature), incomplete stabilization may occur. One conclusion to counter those problems would be to slowly apply the temperature needed for full stabilization. Unfortunately, that method can have significant drawbacks. Stabilization is the slowest of the main steps of carbon fiber production (manufacturing bottleneck), and requires significant amounts of energy to power furnaces for such a long duration [26]. In carbon fiber manufacture, it is ideal to stabilize fibers fully, and as quickly as possible.

Stabilization is affected by many different characteristics of the precursor fiber. As a result, setting optimized stabilization parameters is no easy task. Empirical studies can be performed for each kind of precursor and spinning condition, and find that the optimized stabilization procedure will be different. But in the interest of simplification, the three main parameters that can be optimized for any given precursor polymer are stabilization time, temperature, and tension.

Time and temperature are the drivers for the reactions that take place in stabilization. Knowing the setpoints necessary for the temperature profile ensures that the reactions of cyclization, oxidation, dehydrogenation, and cross linking will occur. Time refers to the rate which the procedure will reach those setpoints, and for how long those setpoints will be maintained, if at all. The time and temperature profile can be broken up into three main phases. The first is the start up ramp to the temperature of the onset of chemical reactions (T_s). The second, is the duration after T_s while the chemical reactions take

place. This is usually a very slow temperature ramp or isothermic dwell. The final stage, after the majority of stabilization reactions take place, is a final temperature ramp where additional cross-linking may occur. In this work, only the first two steps will be observed, as they will provide a strong foundation for further examination in subsequent work.

2.5.2 Temperature Profile up to T_s

The first phase, from start up to the temperature for the onset of the chemical reactions (known as T_s) of cyclization, oxidation, and dehydrogenation, sees a great amount of physical changes in the precursor polymer. Between room temperature and T_s, is the glass transition temperature (T_g) of the polymer. The glass transition is where the fibers change from a brittle to a rubber-like state. (For the homopolymer PAN used in this work, the T_g was @ °C.) After the T_g, the fibers are very compliant, which has the benefit of easy stretching, but also makes them inherently more difficult to handle and process. (Explained in further detail in §2.6)

When analyzing a precursor fiber to find its T_s, one of the most common methods is to use Differential Scanning Calorimetry, or DSC. Since the chemical reactions of stabilization are exothermic, it is simple to find T_s by finding the onset of the first exothermic peak. Other methods for finding T_s have been utilized, including the use of Thermo-Mechanical Analysis, or TMA. By applying a temperature ramp to a precursor fiber, the shrinkage of the fibers can be seen to occur in two distinct steps. The first is the physical entropic shrinkage (recovery from drawing during spinning), and the second is the shrinkage that occurs from the chemical reactions of stabilization. Indentifying the point between the two types of reactions shrinkages is how to find the T_s with a TMA[38]. Another method for finding T_s can also be done by using Dynamic Mechanical Analysis, or DMA. After T_g has passed and the precursor fibers are in the physical entropic recovery stage, the storage and loss modulus values plummet to a mere fraction of the values at room temperature. At the onset of the chemical reactions of stabilization, the storage and loss modulus values begin to climb. The temperature at this onset can also be labeled as the polymer's T_s value.

After finding the value of T_s, finding the temperature ramp up to T_s is the other important aspect to understand from the first phase of the time and temperature procedure. Fitzer et al performed a study on the shrinkage of fiber under differing temperature ramps using thermomechanical analysis. The figure below shows that as the heating rate increased while stabilizing precursor fibers under constant load, the initial physical shrinkage before T_s was not affected. However, the chemical reaction shrinkage after T_s followed a trend of increasing shrinkage as the heating ramp increased beyond 5 °C/min. This was attributed to an increased effect from cross-linking reactions due to the higher temperature ramps[54].

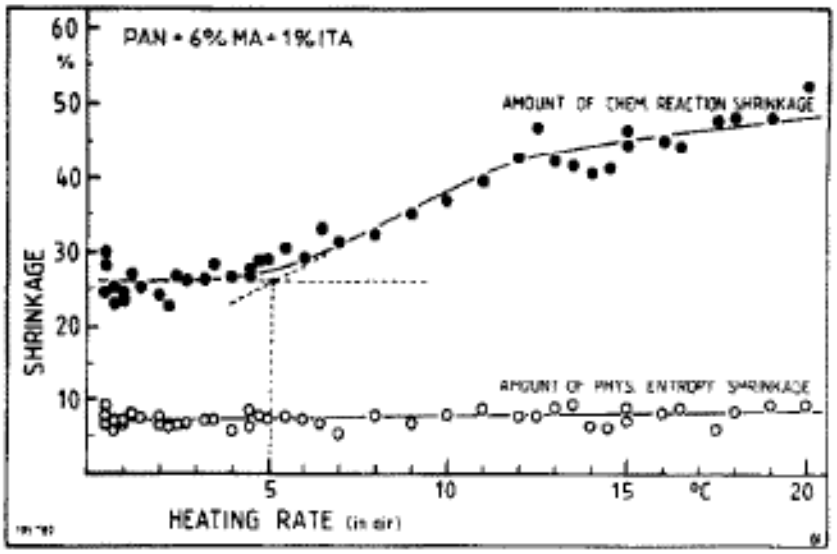

Figure 2-7: Plot of physical entropic shrinkage and chemical reaction shrinkage under various heating rates [38][7]

Shrinkage while stabilizing is to be minimized in order to maintain molecular alignment with the fiber axis (to be explained in the tension section later). Even if the fibers are to be forced from shrinking during stabilization, the chemical reactions that initiate the shrinkage will result in increased tension on the fibers. If stretching (without damage) is to be done in order to optimize final fiber tensile properties, it may be ideal to reduce the

[7] Reprinted from *Carbon* 24-4, Fitzer, E.; Frohs, W; Heine, M., "Optimization of Stabilization and Carbonization Treatment of PAN Fibres and Structural Characterization of the Resulting Carbon Fibres," Pg 387-395, 1985, with permission from Elsevier.

amount of tension incurred from chemical reaction cross-linking. Considering Figure 2-8, if a fiber endured chemical shrinkage or tension associated with a 20 °C/min temperature ramp, the macro-molecular structure may have cross-linked to the point where the fibers cannot be stretched, and the fiber properties can suffer as a result. A maximum heating rate of 5 °C/min is ideal for high modulus and strength carbon fibers[38].

However, what Fitzer's study has shown is that while in the temperature range below T_s, the temperature ramp can afford to be quite fast. Several different researchers have employed this method, where the temperature ramp up to the onset of chemical reactions (T_s) is either very fast, or that phase of stabilization is skipped entirely[40, 66]. Other researchers have gone the conservative route, where more time is taken to stabilize the fiber, reducing the risk of approaching T_s too quickly. From 1 °C/min[67] to Fitzer's 5 °C/min[38].

Regardless of the ramp speed, it should be noted that the ramp speed does have an effect on the temperature value of T_s due to the reaction kinetics of stabilization. Thermal reaction kinetics of PAN precursor show that the slower the temperature ramp, the chemical reaction exotherm will occur at a lower temperature. The faster the ramp, the exotherm will occur later and more pronounced[68].

2.5.3 Temperature Profile After T_s

The second phase for the temperature profile of stabilization is to understand what to do while the majority of the chemical reactions of cyclication, dehydrogenation, and oxidation take place. Starting at the onset of the reactions is the value of T_s. In experimentation, temperature ramps after T_s have ranged from isothermal segments, to slow ramps, to any mixture of stepwise combinations of ramps and isothermal segments[38, 40, 44, 55, 66, 67]. But they mainly share a few priorities in common.

First, the exotherm period after T_s must prevent the fibers from overheating. One of the most difficult aspects of the chemical reactions of cyclization, oxidation, and dehydrogenation is that they are exothermic, and the more aggressive the temperature

ramp during this period, the stronger the exothermic reaction will be. Too strong of a reaction can easily result in the fibers fusing together or burning. The most prevalent method to counter this effect is to slow down the temperature ramp after T_s has been reached. Some methods incorporate stopping the temperature ramp altogether and allow the chemical reactions to take place under isothermal conditions. This is a safe method to use, but unfortunately is also very time consuming. Comonomers allow for a more aggressive temperature profile, as they aid in the initiation of the chemical reactions. However, when stabilizing homopolymer polyacrylonitrile, an isothermal or very slow temperature ramp approach is more appropriate, considering the stabilization reactions happen suddenly and aggressively as compared to copolymers.

Second, the reactions need to take place in a complete manner. A fiber that has been partially stabilized will produce significantly weaker carbon fibers. Cyclization may not have occurred fully, or oxidation and dehydrogenation reactions may have been limited due to lack of time for adequate diffusion of oxygen. Both of these scenarios will result in fiber that will have low carbon yield after carbonization, and produce weakened fibers. On the other hand, in an effort to alleviate one of the slowest steps of carbon fiber production, it is best to do this process as expediently as possible.

Much research has been done to study this crucial period of the stabilization process, including this work. It is a major influence over the final carbon fiber properties, as well as manufacturing costs, as this step is the most time consuming and drives high energy costs. In others' research, this step of the stabilization process has taken anywhere from 10s of minutes operating at 1.0 °C/min [54], to 1.5 - 2.5 hours at 0.56 – 0.89 °C/min[40], to over four hours with an isothermal dwell [66]. Some of the major contributors to this variation include, general inconclusive understanding of the process parameters, precursor fiber chemistry, crystalline structure, and other precursor fiber characteristics.

Knowing when the fibers have been fully stabilized can be difficult to ascertain, and a number of researchers have followed numerous standards. Using a DSC has been one of the most common tools for finding the temperature value for T_s, especially in how it is

affected with different temperature profiles (reaction kinetics) and is also helpful in finding the temperature of additional cross linking as seen in the second distinct exothermic peak [66]. It has been used with and without nitrogen atmospheres to separate the reaction of cyclization from the other oxidative reactions. Using a DMA, storage and loss moduli have been used to distinguish the completeness of reactions, where increasing storage modulus has been attributed to cyclization and additional cross linking, and the loss modulus increases with the destruction of PAN crystals and decreases with cross linking. TGA has been useful for singling out reactions and for clarifying the reactions seen with other instruments. Oxygen takeup has also been studied using the TGA[69]. Shrinkage behavior has also been observed with the TMA to study the reactions during stabilization [54, 66]. Additionally, FTIR has been an essential tool for calculating the completeness of stabilization. It has the ability to provide a snapshot of a fiber's chemistry, and with that has arisen the use of the stabilization index and the ring closure index, which can express the degree of important aspects of stabilization with a dimensionless ratio [66, 70]. To define those ratios, the stabilization index (E_s) is the absorbance peak for carbon-carbon double bonds (1600 cm^{-1})over the peak for nitrile (2240 $cm^{-1)}$, the ring closure index being the value of the absorbance peak of the double bonds over two times the value for the nitrile[70]. Because such a variety of methods exist, there still exists some uncertainties whether the evidence showed by a method can be conclusive[71].

The above mentioned instruments have been crucial to the study of the stabilization of PAN fibers, and decades' worth of correlations have been made between these results and the ultimate tensile properties of the final product. But one caveat remains; despite the enormous amount of study that has been made to connect these experiments, the seemingly endless amount of variation in the precursor fiber characteristics makes the study of fiber stabilization a difficult task. What can be taken from the lessons of previous research, however, are the tools necessary to move forward with any new precursor fibers and any new stabilization manufacturing methods to optimize for the end-users' needs.

2.6 Stabilization Factors that affect Carbon Fiber Quality: Tension

2.6.1 Introduction

As mentioned earlier in this work, PAN based carbon fibers saw rapid development and increased tensile properties when stretching was applied to the fibers during stabilization. Shrinkage is undesirable for precursor fibers in the stabilization process. Linear alignment of the polymer chains is desirable. If shrinkage occurs, the internal structure of the fiber loses that crucial alignment. Similar to the spinning process of creating the precursor fiber from polymer solution, it is desirable to stretch while stabilizing.

2.6.2 Understanding Shrinkage

Before moving into the topic of stretching during stabilization, it is helpful to understand what happens to fiber during stabilization when little to no load is applied to the fibers. There exists two different and rather distinct phases of fiber shrinkage that occurs doing stabilization: physical and chemical.

First, physical shrinkage is seen during the early phase of stabilization, which is attributed to entropic recovery of a drawn and quenched material. Internal stresses incurred from stretching during spinning of the precursor fiber will be relaxed when the fiber is heated. This is based on the helical structure of the PAN molecule where there exists intermolecular repulsive forces between nitrile group dipoles [44]. Fitzer et al [54] as mentioned earlier from their TMA studies, found that regardless of heating rate, the amount of physical shrinkage was constant for a given polymer, which indicates that the amount of physical shrinkage may be a function of the spinning conditions and the macro-molecular structure of the precursor fiber.

Secondly, there is chemical shrinkage. This shrinkage occurs during the stabilization reactions, which take place at a distinct temperature range above that of the physical entropic shrinkage stage. The reaction of cyclization, due to the formation of the cyclized ladder structure, is the sole contributor to the chemical reaction shrinkage[43]. The amount of shrinkage during this phase of stabilization can be affected by many factors, namely fiber chemistry, orientation, and the energy diffusion into the fiber tow (which is affected by the user parameters such as temperature profile)[72]. The study done by

Fitzer[54] showed no effect of temperature profile to physical shrinkage, but there was a very strong relationship between the temperature ramp and the resulting chemical reaction shrinkage.

2.6.3 Stretching During Stabilization

Stretching during stabilization is an important tool for optimizing fiber properties. The increased intermolecular movement of stretching during increased temperatures allows for more ease of cyclization[44]. Additionally, *in situ* stretching reduces imperfections such as small bubbles and pores that may have resulted during the spinning process, further improving the final properties of the carbon fiber[11].

The best time to do the majority of fiber stretching is between the temperatures of the glass transition (T_g) and the onset of stabilization reactions (T_s). Wu et al studied draw ratios to find that the contribution of stretching at higher temperatures provided little benefit to the final properties, as the stabilization reactions have fixed the structure of the fibers [43]. Yet stretching earlier, proved to change the orientation of the fiber structure, especially in the amorphous region. This allowed for reduced chain scission and lower loss of molecular alignment, and significant changes in the cyclization reaction of the fiber [43].

Then there is the question of how much strain that should be applied to fibers during stabilization. This is very much dependent on the characteristics of the precursor fiber. Precursor fibers of the same polymer composition will have different stretching potential during stabilization if one endures more stretching during spinning. Fibers that undergo the same spinning conditions will have different stretching potential during stabilization if they have different polymer compositions. Variations in the above mentioned parameters can have such a significant impact largely because they affect the molecular structure of the precursor fiber.

Either when stretching generously just after the glass transition or lightly during stabilization, it is possible to stretch too much. Understanding can be best described generally with the changes to the fibers' macro-molecular structure of the quasicrystal

and amorphous regions. One study performed by Lian et al went into detail with stretch and recovery tests along with Wide Angle X-Ray Diffraction, FTIR, and DSC, to identify what stretching does to each type of region. With no stretching, it was seen that both regions lose some orientation[44]. Initially, light stretching may have little to no impact on the amorphous PAN chains while providing slight elastic orientation of the quasi-crystal regions. In more moderate stretching, a majority of the changes are in the amorphous region as it experiences elastic-dominated orientation due to deformation, while the quasi-crystals endure plastic extension, along with growth[44]. At higher draw ratios, the amorphous chains and quasi-crystals respectively experience elastic and plastic extension, or slippage[44]. It is in that highest range of draw ratios that the tensile strength of the resulting carbon fibers decreased, and increases to the modulus were significantly diminished[44]. This is attributed to the quasi-crystalline region being damaged and torn apart due to slippage. Therefore it is possible to overdraw the precursor fibers in the compliant temperature range.

3 CHARACTERIZATION OF PRECURSOR FIBER AND STUDY OF STABILIZATION REACTIONS

3.1 Introduction

The final properties of carbon fiber depend on an exceptional number of variables. Not exclusive to the parameters set in stabilization, but the spinning of the precursor fiber and the carbonization of stabilized fiber have significant effects on the ultimate properties of carbon fiber. Moreover, many of those variables in the manufacture of carbon fiber are heavily inter-dependent on each other. A cascading effect can be seen, where polymer formulation can change the necessary parameters to spin high quality precursor fibers, where those conditions ultimately change the optimized parameters to stabilization, and the process continues for carbonization. Therefore, it is prudent to explain the manufacture and the properties of the precursor fibers used for this work. After the review of the making of the precursor fiber, the investigation into the reaction kinetics of the fibers will be performed.

3.2 Spinning of the Precursor Fiber

3.2.1 Introduction

Precursor fibers used in this thesis were spun in-house at the University of Kentucky Center for Applied Energy Research (UKCAER) from dope formulated from commercially available homopolymer polyacrylonitrile in solution with N,N-dimethylacetamide (DMAc).

3.2.2 Parameters Used for Spinning Precursor Fiber

Homopolymer PAN was made into a 18 wt% solution in DMAc (also called dope). The dope was made in an airtight, heated mixer with stirring capabilities and kept sealed until needed. During spinning, the polymer was extruded through a 100 filament die. The wet-spun fibers were spun with a total draw ratio of 5.94.

The spinline contained 9 baths in total, with controlled stretching between each bath. After the final bath, fibers travelled through a series of heated rollers for the purpose of

drying, and then were taken up on a cardboard core with a traversing pulley arranging the tow. Below are the parameters used for the spinning of the fibers.

Table 3-1: Summary of Spinning Conditions for Precursor Fiber

Bath	Bath Temp. °C	Bath Concentration wt% DMAc in water	Draw ratio thru bath
Coagulation			
1			
2			
3			
4			
5			
6			
7			
8			
			*
			**
		Total DDR	5.94

*Heated Roller
**Collector

After the precursor fibers were spun by the above method, a portion of the fibers were stretched further in a heated glycerol bath. This allowed for two sets of fibers, with identical dope formulation and spinning conditions, with the exception of one added glycerol stretching step. This would allow for studies to compare between two precursor fibers with different stretch ratios. The difference in stretch ratio will, in turn, result in a difference of diameter and alignment of the PAN molecules.

Post spinning glycerol stretching was performed in a bath of glycerol heated to 170 °C with a draw ratio of 1.8, followed by a rinse in near boiling water. No stretching was performed in the hot water bath. As a result, the glycerol stretched fibers had a total draw ratio of 10.69.

3.2.3 Diameter Measurement of Precursor Fiber

Samples of the spun precursor fiber were collected and bundled for diameter measurement. Fibers were placed vertically in a small cylindrical mold where epoxy was

filled and cured such that the fibers were coaxial with the cylinder of epoxy. The sample was then sanded and polished so that the fiber ends would be exposed with no blemishes. Optical microscopy pictures were taken and analyzed for (equivalent circular) diameter measurement.

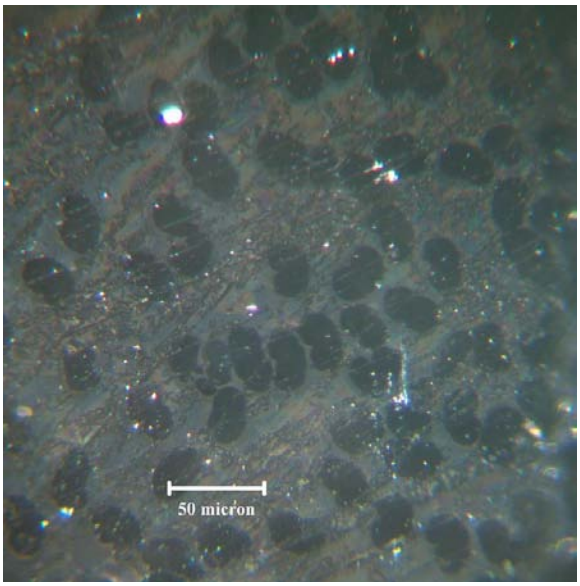

Figure 3-1: Optical microscope image of precursor fibers

The cross-sectional shape of the precursor fibers were not perfectly cylindrical, consequently, direct diameter measurement would not be suitable. The outlines of the fibers were analyzed resulting in the output of fiber perimeter and enclosed area. With area measurements, equivalent circular diameters were calculated. The assumption is that calculating the diameter of a circle with the same area as the fiber would be more accurate and consistent than the average of several diameter measurements spanning on each fiber cross section.

$$ECD = \sqrt{\frac{4 * A}{\pi}}$$

Where ECD is equivalent circular diameter and A is the area of the measured fiber. Additionally, circularity was measured. Circularity is the ratio of the area of the measured fiber to the area of a circle with the same perimeter as the fiber.

$$C = \frac{A_f}{A_c}$$

$$C = \frac{A_f}{\frac{\pi P^2}{4\pi^2}}$$

$$C = \frac{4\pi A_f}{P^2}$$

Where C is the circularity, A_f is the measured fiber area, P is the measured fiber perimeter, and A_c is the circle area with the same perimeter. The results of the spun precursor are in Table 3-2.

Table 3-2: Precursor Fiber Diameter and Circularity

	Area (micron²)	Equivalent Circular Diameter (micron)	Perimeter (micron)	Circularity
Avg	460.13	24.15	101.61	0.56
Std Dev	61.56	1.65	7.45	0.03

Number of Samples: 31

As for the glycerol stretched fibers, the same process was performed to study their diameter and circularity. Below is a cross-sectional image of those fibers.

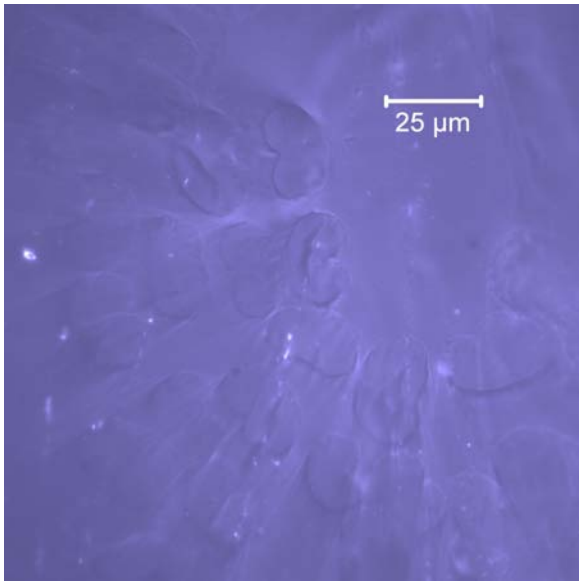

Figure 3-2: Optical microscope image of glycerol stretched fibers

After performing measurements similar to the regular precursor fibers, the area and circularity characteristics were found.

Table 3-3: Glycerol Stretched Precursor Fiber Diameter and Circularity

	Area (micron²)	Equivalent Circular Diameter (micron)	Perimeter (micron)	Circularity
Avg	335.149	20.60	86.411	0.56
Std Dev	51.082	1.57	6.369	0.02
	Number of Samples: 38			

It should be noted that after glycerol stretching, the fibers maintained their circularity. Taking the fibers beyond their glass transition and inducing stretching did not alleviate any of the bean shaped characteristics of the original fiber, as the cross-sectional profile of the fibers are typically set in initial coagulation.

3.3 Thermal Characterization

3.3.1 Introduction

In order to create a starting point for the study of stabilization, DSC studies were performed to study the reaction exotherm of cyclization and dehydrogenation. By performing the tests under an array of temperature ramps, reaction kinetics can be observed.

3.3.2 Differential Scanning Calorimetry and Reaction Kinetics

One of the first and most basic studies that can be performed on a precursor fiber is to find its activation energy, i.e. the minimal energy needed to initiate the reactions of stabilization. Then that information can be used to build the Arrhenius equation to describe the dependence of the rate constant of a reaction to the temperature. The Arrhenius Equation is:

$$k = Ae^{-\frac{E_a}{RT}}$$

Where k is the rate constant of a reaction (1/s), A is the frequency factor (1/s), E_a is the activation energy (kJ/mol), R is the gas constant (8.314 J/(mol*K)), T is absolute temperature (K).

Not knowing the rate constant, the frequency factor, or the activation energy, other tools to study reaction kinetics need to be utilized. A common method is to determine the material's activation energy through experimental methods, including the use of differential scanning calorimetry.

DSC studies were performed on the precursor fibers of both draw ratios (5.9 and 10.7 DDR). Activation energy values were obtained by studying the temperature recorded at the peak of exotherm, as described in reaction kinetics methods by Kissinger and Ozawa. Kissinger's equation is as follows:

$$-\frac{E_a}{R} = \frac{d\left[ln\left(\frac{r}{T_p^2}\right)\right]}{d\left(\frac{1}{T_p}\right)}$$

[68]

Below is the equation used to find activation energy with Ozawa's method:

$$-\frac{E_a}{R} = 2.15\frac{d[log(r)]}{d\left(\frac{1}{T_p}\right)}$$

[73]

Where E_a is activation energy (kJ/mol), R is the gas constant (8.314 J/(mol*K)), r is the heating rate (K/min), and T_p is the absolute temperature at exothermic peak (K).

3.3.3 Method and Materials

For this experiment, a TA Instruments Q100 series DSC was used. Samples were run under constant heating rates of 1.0 °C/min, 2.5 °C/min, 5.0 °C/min, 10.0 °C/min, and 20 °C/min. All ramps started at 30 °C and ended at 400 °C. Sampling rates were kept at one sample per second for all heating rates, with the exception of a sample rate of five seconds/sample for 1.0 °C/min.

Samples were prepared by taking an approximately 3 meter length of 100 ct tow of precursor fiber and folding it in half repeatedly until the tow reached a length of about 10 cm, creating a thicker tow of several thousand fibers. The ends were trimmed and the fibers were tightly bundled. A fresh razor blade was used to slice off approximately 1 mm of the fiber tow. This was then repeated in order to achieve a sample size around 4.5 to 5.5 mg. Samples were loaded in aluminum pans, where the lids were perforated in four places in order to ensure that the sample would be supplied enough oxygen while

testing in the air atmosphere, while allowing for proper heat transfer of the sample from the lid to the sample pan. All sample lids were crimped to the pans in order to ensure good thermal contact.

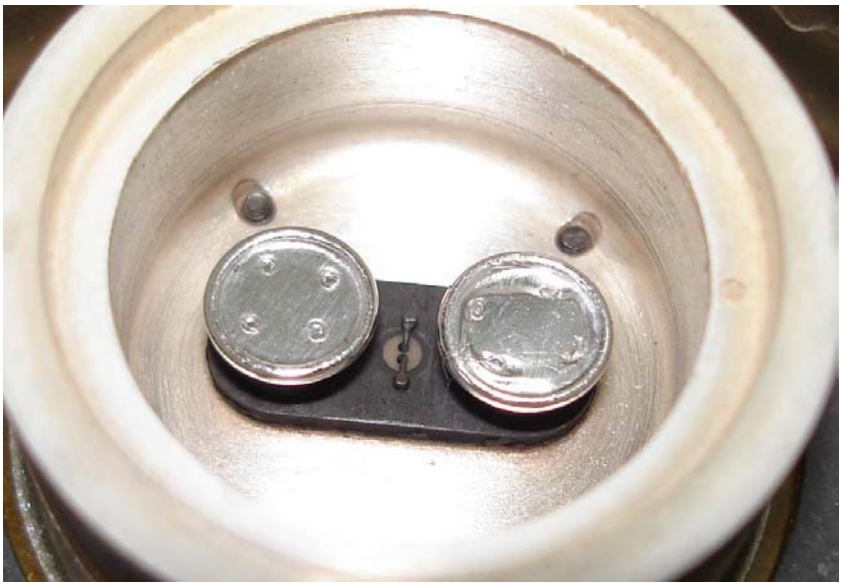

Figure 3-3: Sample pan and reference pan loaded in DSC

3.3.4 Results

The temperatures at the peak of exotherm were recorded. The values of fiber samples of both draw ratios at each heating rate can be seen below.

Table 3-4: DSC Temperature at Exothermic Peak

	DDR	
	5.9	10.7
Heat Rate (°C/min)	T_{peak} (°C)	T_{peak} (°C)
1		
2.5		
5		
10		
20		

Corresponding those temperature values and ramps are the plots to find the activation energies with the Kissinger and Ozawa method. Below are their respective plots.

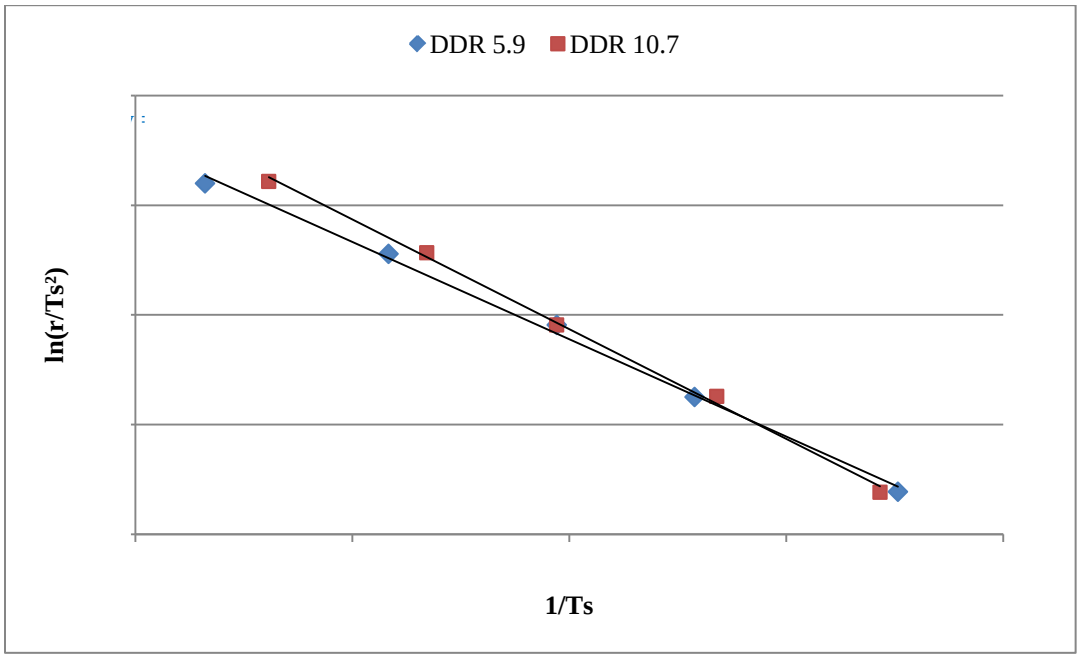

Figure 3-4: Plot according to Kissinger Equation

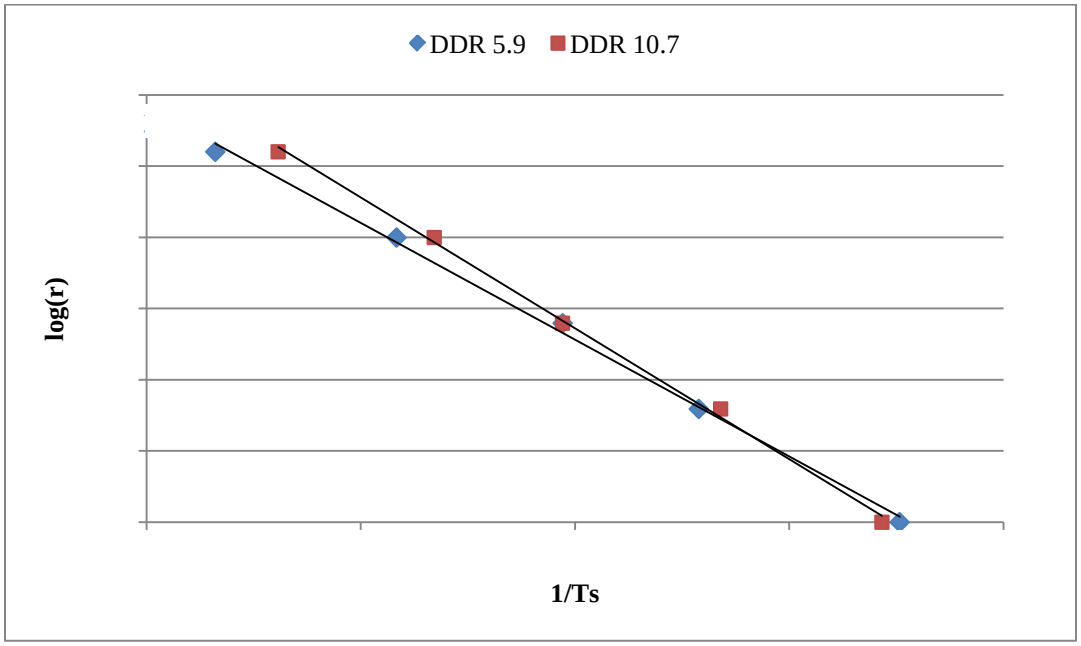

Figure 3-5: Plot according to Ozawa Equation

Fitting the data to linear trend lines and solving for activation energy and frequency factor, the final results can be seen below.

Table 3-5: Activation energy and frequency factor values for precursor fibers of both draw ratios

	Kissinger		Ozawa	
DDR	5.9	10.7	5.9	10.7
Activation Energy, E_a (KJ/mol)	147.6	166.5	146.7	164.3
Frequency Factor (1/min)	7.43E+12	4.85E+14	6.14E+12	3.03E+14

The activation energy and frequency factor values between both the Kissinger and Ozawa methods are very similar. However, the values between the two different draw ratios of homopolymer PAN showed a significant difference, where the glycerol stretched fibers had a higher activation energy.

3.4 Conclusion

Eighteen wt%-homopolymer PAN was made into a dope with DMAc and wet-spun with a total draw ratio of 5.9 resulting in fibers with a diameter of 24.15 microns. A portion of that fiber was then glycerol stretched to form a precursor fiber with a total draw ratio of 10.7 and an equivalent diameter of 20.60 microns. Both fibers were then characterized in the DSC to observe the activation energy and frequency factor values using both the Kissinger and Ozawa methods. The 5.9 DDR precursor fiber had an activation energy of 147.9 kJ/mol, lower than that of the glycerol stretched fibers that had an activation energy of 166.5 kJ/mol (citing Kissinger numbers). This stands in contrast with previous work mentioned [50], where post spinning stretching lowered the activation energy and initiation temperatures, and where post spinning stretching resulted in higher orientation and crystallinity along the fiber axis, leading to improved properties[69]. However, in those works, comonomers were used, and may not be directly applicable to the homopolymer PAN used in this study.

Without further research, some hypotheses to explain this phenomenon are proposed. The higher stretch ratio may have increased the molecular crystallinity of the fibers to the point where disordered regions that allow for the initiation of cyclization became the limiting factor in overall stabilization reactions. And if the quasi-crystalline regions were damaged due to excessive stretching, the propagation of the cyclization reaction may

have been interrupted more compared to the lower draw ratio fiber with less damage. Further work to study this phenomena could include a temperature ramp in a nitrogen environment to isolate cyclization, then repeated in air to observe dehydrogenation and cross linking separately. Finding the activation energy of dehydrogenation can study the effect of the change in diameter and surface area to volume ratios and how it would affect oxygen diffusion into the fibers. Isolating cyclization would also be beneficial to see if its activation energy increased with the drawing of the precursor, to back up the conclusion made in this work. Additionally, further studies with wide-angle X-ray diffraction could confirm the assumptions made on the crystallinity of the precursor fibers. Another thought to explain the higher activation energy would be to gain further understanding of the tacticity of the PAN molecules. If the chains were highly syndiotactic, aggressive stretching of the amorphous polymer chains could result in a higher activation energy for the nitrile groups to cyclize.

Moreover, it is important to note that the studies referenced that saw reduced activation energies with increased stretching were fibers that were half the diameter of the ones in this study, and also included fibers with comonomers. The lack of decreased activation energy due to increased stretching may be a function of the fibers used in this study. The stretching ratio of 1.8 DDR may have been too aggressive on the large homopolymer PAN fibers, and resulted in more slippage and breakages within the fiber molecular structure, especially in the quasi-crystalline regions, resulting in generation of defects. Testing an array of different stretch ratios may have shown that glycerol stretching at 1.8 DDR was damaging and lower draw ratios could be beneficial. Additionally, with the fibers being homopolymer, no comonomers were available to ensure adequate amorphous regions to initiate cyclization. With a higher draw ratio, these fibers' macro-molecular structures may be more crystalline, to the extent that cyclization may have been impeded. Since dehydrogenation prefers to take place on cyclized polymer chains, the cyclization mechanism may have been the dominate impediment to stabilization. In order to confirm this, studying the degree of crystallinity between the two precursors would be helpful.

4 STATE OF REACTION DURING STABILIZATION: OPTIMIZATION OF THE TEMPERATURE PROFILE

4.1 Introduction

Beginning with the study of reaction kinetics in the previous chapter, more work is necessary in order to study the optimum temperature profile for a given precursor fiber. Different methods and instruments for thermal analysis during stabilization have been mentioned in the literature review portion of this work, and the primary means for studying stabilization will be through dynamic mechanical analysis (DMA). Holding stabilizing fibers in isostrain conditions while observing stress will be performed in a matrix of different temperature profiles. Then some of those procedures will be carried out and tested in batch production of carbon fibers, testing for tensile properties of the final product.

4.2 Optimizing the Temperature Profile – Linking Temperature Profile to *in situ* Stress

4.2.1 Introduction

Optimizing the temperature profile of any given precursor fiber has been the subject of much research and has been done using a multitude of instruments and methods. Of the instruments and procedures available to study the temperature profile of PAN fiber stabilization, Dynamic Mechanical Analysis will be used under non-oscillatory isostrain conditions to observe in-situ stress of the precursor fiber. The goal was to find any relation between the *in situ* stress profile and the fiber properties.

Stress-isostrain tests were preferred for the main reason that isostrain conditions will prevent significant macro-molecular changes that may occur if the fibers were allowed to shrink. This will provide results more relatable to the study of the current methods used for batch stabilization, and ultimately create a baseline that will be applicable to the construction of a continuous stabilization line, as it will be controlled by velocities and draw ratios, not stress (stress controlled, as in, DMA oscillatory measurements).

4.2.2 Method and Equipment

A TA Instruments Q 800 Dynamic Mechanical Analysis (DMA) was used. Set to maintain isostrain without any oscillatory motion, the DMA recorded stress endured by the fibers as they underwent a matrix of different temperature profiles.

Figure 4-1: TA Instruments Q800 series DMA

Sample preparation started with taking the 100 count precursor fiber tow and laying the bundle across a sheet of paper, then securing at the ends. Paper frames with 10 mm openings were slid under the fiber tow, where the fibers were glued to the frame with Epoxy. Frames were then mounted to the tension clamps of the DMA, ensuring that the clamps were biting to the adhesive and not directly on any fibers. The clamps were tightened to three inch-pounds of torque. The air bearing to the DMA was then locked and the sides of the paper frame were trimmed away, leaving a prepared sample ready to be tested.

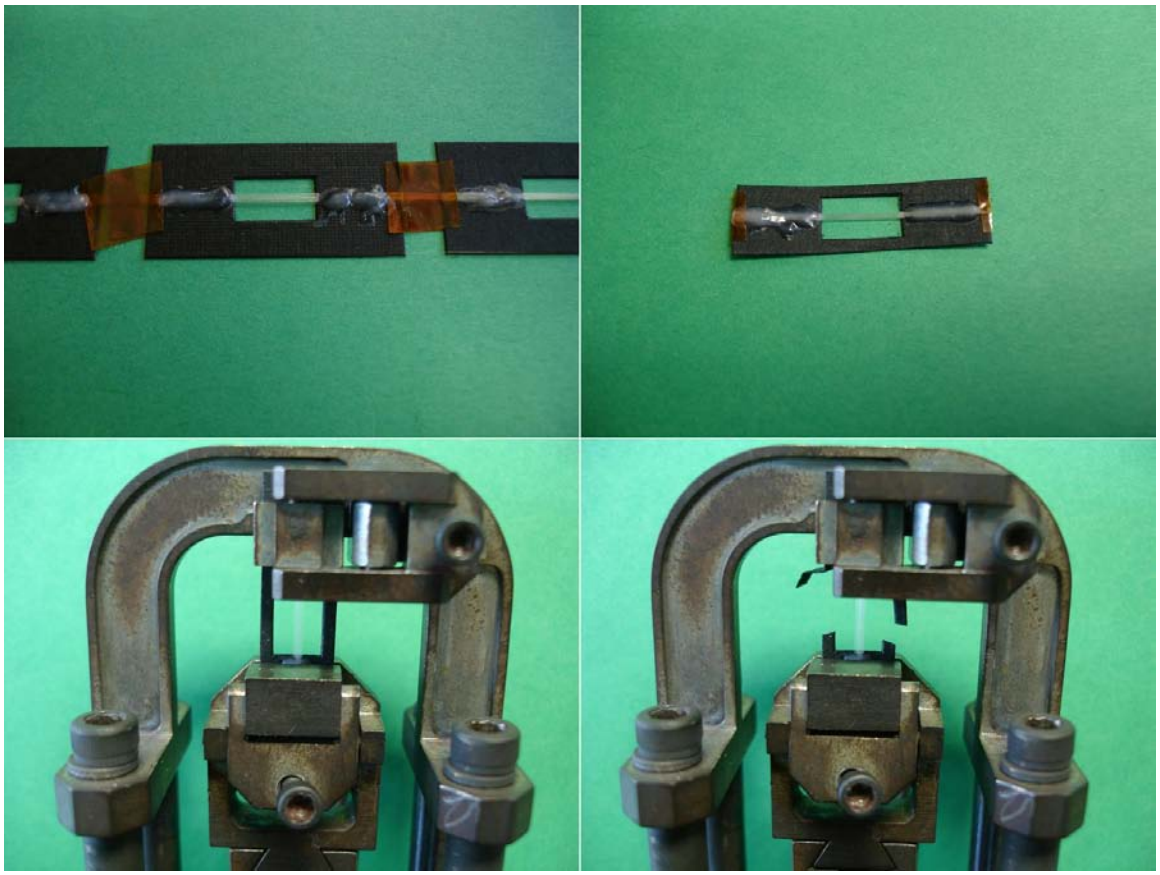

Figure 4-2: (clockwise from top left) Row of samples mounted and glued; Frame removed from fiber tow and ready to mount; mounted fiber frame in tension clamp of DMA; sides of frame trimmed and moved

The testing matrix that was established was based on results of the DSC experiments from Chapter 3. The initial ramp from ambient temperature was set to 5.0 °C/min. This was based on the work of Fitzer et al [54] finding that physical shrinkage was not influenced by the temperature ramp, but shrinkage due to the stabilization reactions saw a pronounced increase beyond the heating rate of 5 °C/min. Although the initial temperature ramp does not cover the temperature needed for cyclization initiation (T_s), once the ramp is ceased and the next ramp begins, the reactions during the second ramp will not be overly influenced by the reaction kinetics of the first ramp. Additionally, the TA Instruments Q 800 specified that due to the chamber size and thermal mass of the mounting clamps, 5.0 °C/min is the most aggressive ramp that can be used without experiencing a thermal lag between the set point temperature and the actual temperature.

At 5 °C/min, the temperature at the onset of the reaction exotherm from the DSC studies was @ °C. Temperatures selected to be the end of the initial heating ramp (denoted T_s*) were taken in @ °C increments of (High) °C, (Med) °C, and (Low) °C. To differentiate, T_s defined earlier was the onset to reactions based on a linear temperature ramp, and T_s* is a user-established temperature for reaction initiation. The user has some control, as slowing the temperature ramp will induce stabilization because of the reaction kinetics. For the final heating ramp after T_s*, three different selections were made of (Slow) °C/min, (Moderate) °C/min, and (Fast) °C/min. Ramps were not selected to be more aggressive, as the precursor fibers were homopolymer PAN, which endures a quick and aggressive reaction exotherm, and is prone to coalescing and burning at faster heating rates. All tests were carried out until the observed stresses had reached steady-state.

In summary, the testing matrix can be seen in the table below:

Table 4-1: Testing Matrix for DMA Stress / Isostrain Studies

	T_s* = Low °C	T_s* = Med °C	T_s* = High °C
Final ramp = Slow °C/min	X	X	X
Final ramp = Mod. °C/min	X**	X	X**
Final ramp = Fast °C/min	X	X	X

Three samples tested per level

**Denotes levels selected for batch stabilization, carbonization, and tensile testing.

4.2.3 Results

The objective was to find any correlation between temperature profile, and the maximum steady state stress of the fibers. Time to that maximum stress was also recorded and studied. In addition, the maximum derivative of the stress with respect to time was recorded to study the reaction kinetics of stabilization. Later in this chapter, some of the experimental levels were batch stabilized to those parameters, carbonized, and tested for tensile properties.

A typical result of three experimental levels shown below, displays the development of stress with respect to time. The temperature profiles shown demonstrate that each of these three samples represent one of the T_s* values (Low, Med, High) °C, and they all have the final ramp of (Moderate) °C/min after T_s*.

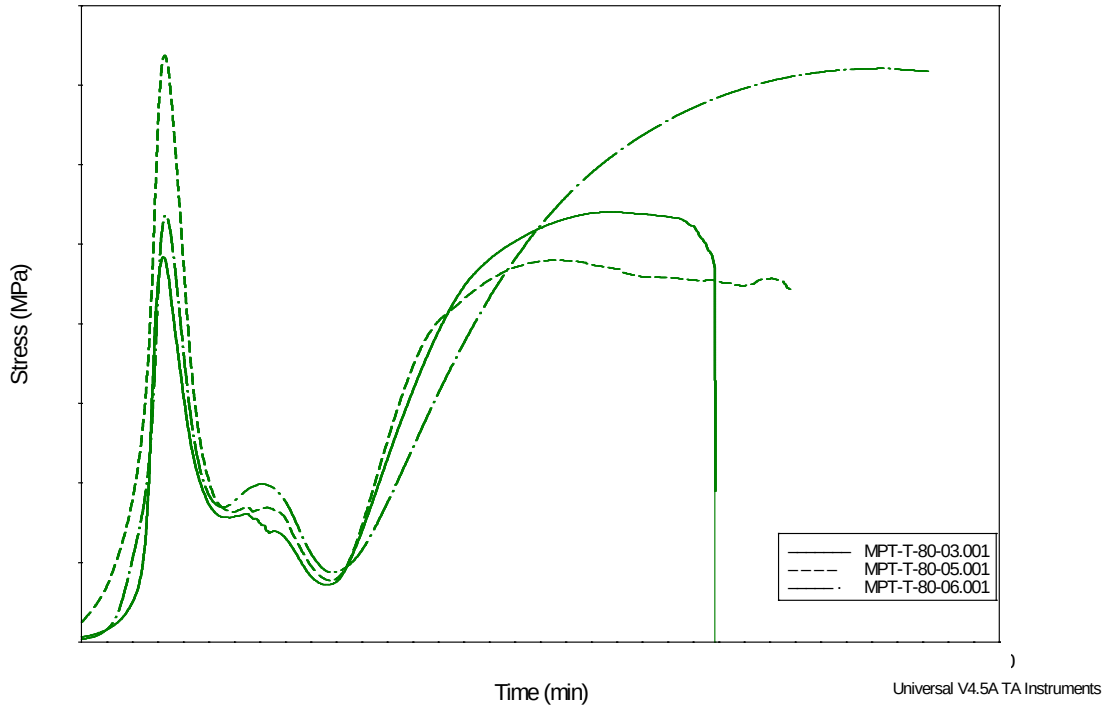

Figure 4-3: Stress results from three samples. Note the highest stress was attained with T_s = (Low) °C, the lowest stress occurred when T_s = (High) °C.

To observe what occurs when the T_s* value is maintained while changing the final temperature ramp, the below example shows a selection of samples where T_s* = (Low) °C and each curve represented one of the final heat ramps (Slow, Moderate, Fast) °C/min.

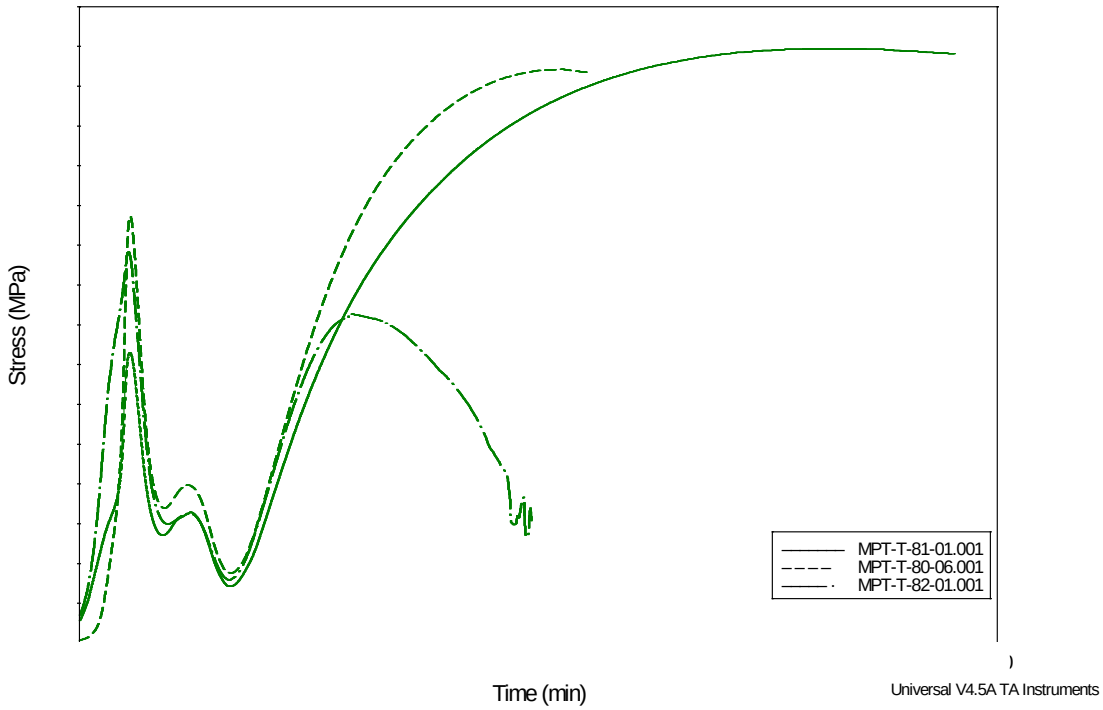

Figure 4-4: Stress results from three samples with differing final temperature ramps. Note the highest stress was attained with h_f = (Slow) °C/min, while the lowest stress occurred when h_f = (Fast) °C/min.

The above mentioned figures are two examples of one array along the experimental matrix. Three samples were tested for each test level, averaged, and summarized in the table below. Included is the data taken from the maximum time derivative of each stress curve, along with the time associated with that maximum.

Table 4-2: Summary of data from stress observation while in isostrain conditions in DMA

	Final Temperature Ramp		
	Ts value	Ts value	Ts value
Peak Stress (MPa)			
STD DEV			
Time at Peak Stress (min)			
STD DEV			
Peak δσ/δt (Mpa/min)			
STD DEV			
Time at Peak δσ/δt (min)			
STD DEV			

First observation should be paid to the peak stress and time to peak stress. As it was alluded to in the figures above, the max stress and time to max stress is dependent on the temperature profile. The figure below will provide some graphical representation of the table above.

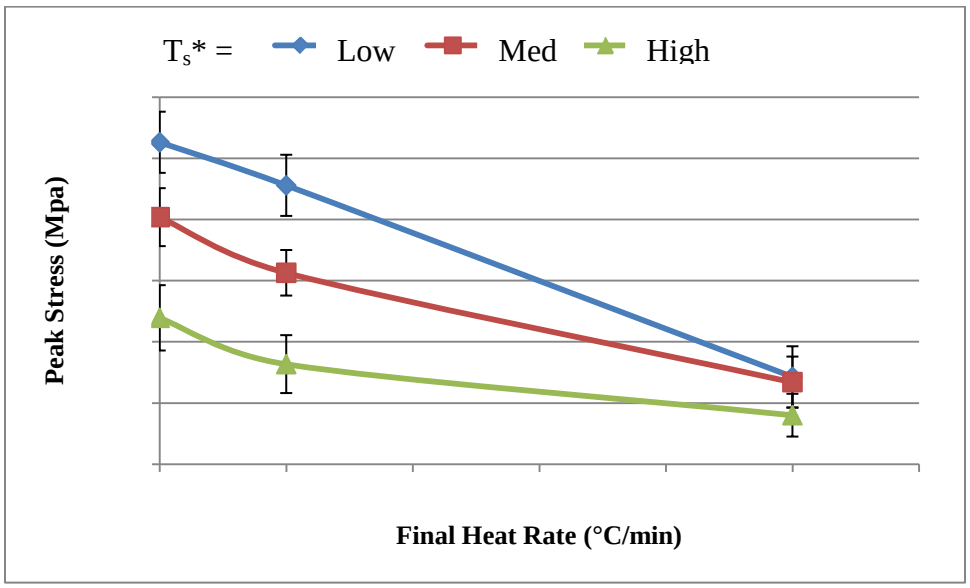

Figure 4-5: Peak Stress vs Final Heat Rate

When observing the peak stress as a function of the final heating rate, each T_s* value saw an upward trend in peak stress as the final heat ramp got slower. The highest stress was obtained through the (Low) °C T_s* value followed by (Slow) °C/min conditions, and the lowest maximum stress occurred when T_s* was (High) °C followed by a (Fast) °C/min temperature ramp. In short, the more aggressive the temperature ramp, the lower the max

strain, the more conservative the temperature ramp, the higher the max stress. That conclusion is by no means global in scope, it only applies to the limited temperatures and ramps considered in this study. For example, if the temperature profile could not allow the fibers to reach the activation energies of the stabilization reactions, or the temperature ramp could be so aggressive the fibers quickly coalesce and melt.

To observe these trends differently, exchanging the three data sets with the x-axis values shows how the peak stress was affected by the selection of the T_s* value.

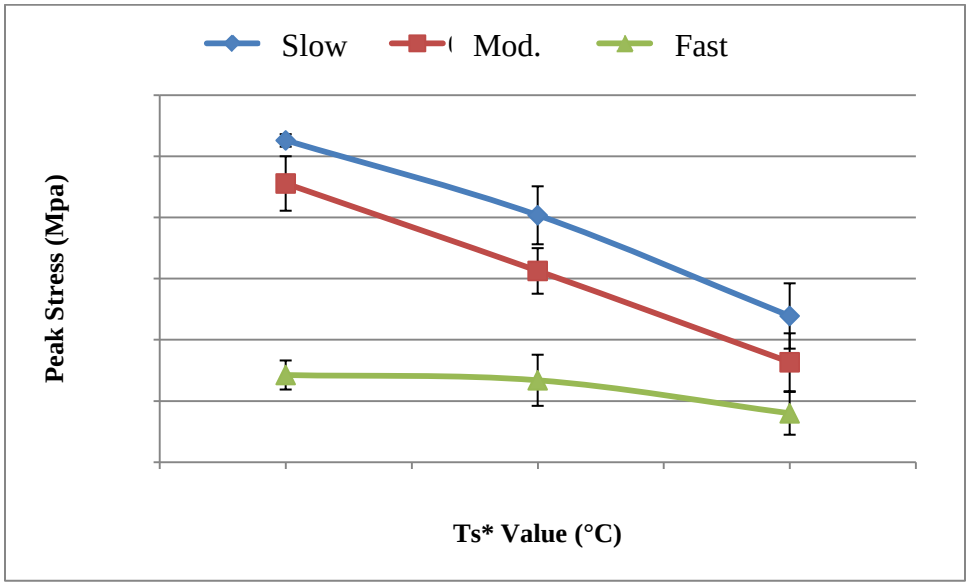

Figure 4-6: Peak Stress vs T_s* Value

In the plot comparing peak stress to the selected T_s* value, it can be seen that (Fast) °C/min resulted in the lowest peak stresses. Additionally, the observed trend of peak stress throughout the three T_s* values shows that the slower second heating rates have an upward trend with lower selected T_s* values, however, that is not the case for the more aggressive (Fast) °C/min. Despite changing the T_s* value, a negligible effect can be seen on the maximum observed stress. This indicates that the selection of higher temperature heating rates should be lower than (Fast) °C/min if steady state stress is any indicator for final carbon fiber properties.

The second major observation from the table should be the time that was needed to reach the peak stresses. Time to peak stress was also considerably affected by the temperature profile.

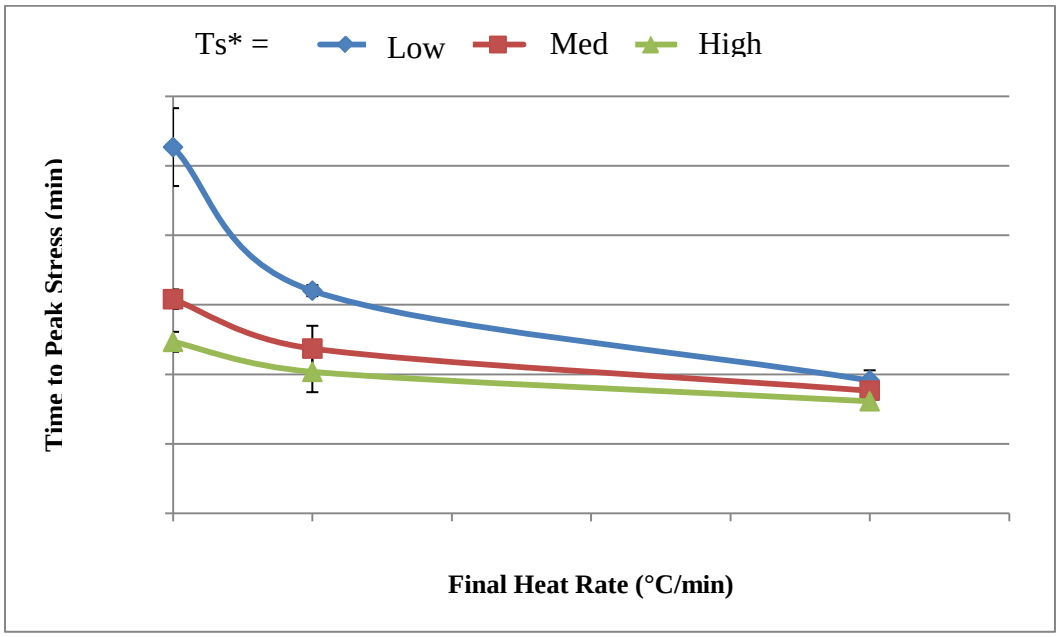

Figure 4-7: Time to Peak Stress vs Final Heat Rate (time relative from start)

As seen in the figure above, as the final heating rate slows, the time that is needed to reach the maximum stress markedly increases. And the lower the T_s* value, the time change is more pronounced among the three final heating rates. Most significantly, along the temperature profiles that had T_s* = (Low) °C, the times to peak stress went from @ min, to @ min, to @ min (relative to start time). And if the peak stress values were included with those numbers, @ min to @ MPa, @ min to @ MPa, @ min to @ MPa, it can be observed that with over @ more minutes of time under temperature (a @ % gain), the fibers only ultimately gained an @ % increase in peak stress.

In addition to observing the maximum stress and time needed to reach that stress value, another data point considered was the maximum derivative of stress with respect to time. When observing the maximum slope for the stress, a dependency on the T_s* value was evident, as well as the final heating ramp. Each T_s* value had a similar profile, where a marked increase was seen between (Slow) and (Moderate) °C/min final heating ramps,

and with little change seen between (Moderate) and (Fast) °C/min. The exception is that each T_s* value would offset that profile by approximately @ MPa/min, where the higher the T_s*, the steeper the slope of the developing stress in the stabilizing fibers. This can be seen in the figure below.

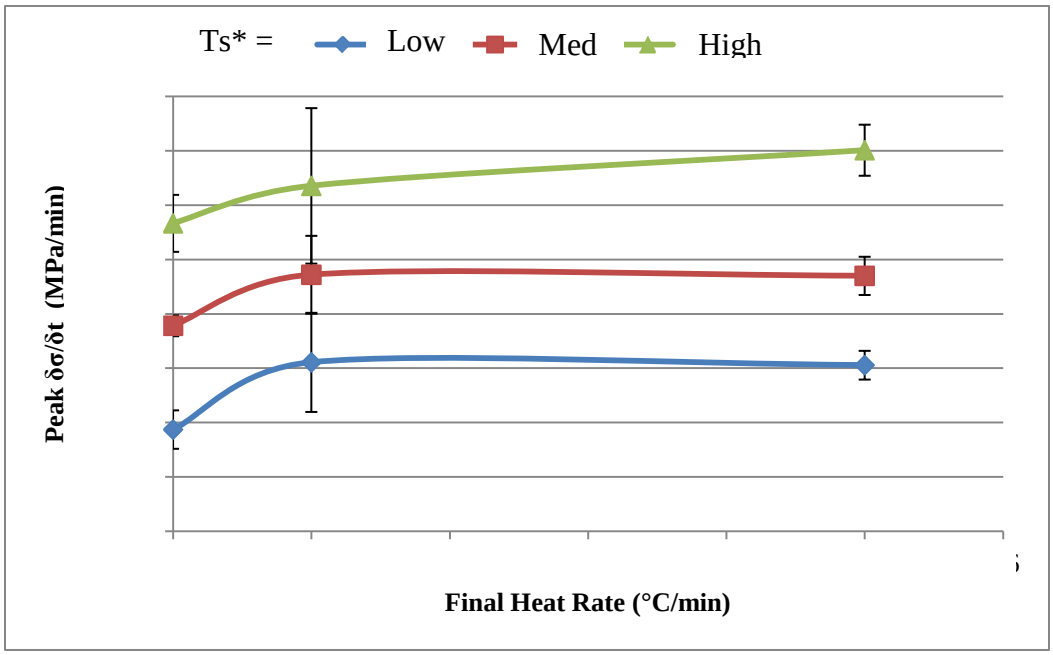

Figure 4-8: Peak δσ/δt vs Final Heat Rate

As for the time associated when the peak slope in the stress occurs, it has been found to be mainly dependant on the value of T_s*. For all samples, immediately after T_s* has passed the stress will start to rise. The difference between (Slow) and (Fast) °C/min is negligible compared to the effect of T_s* value.

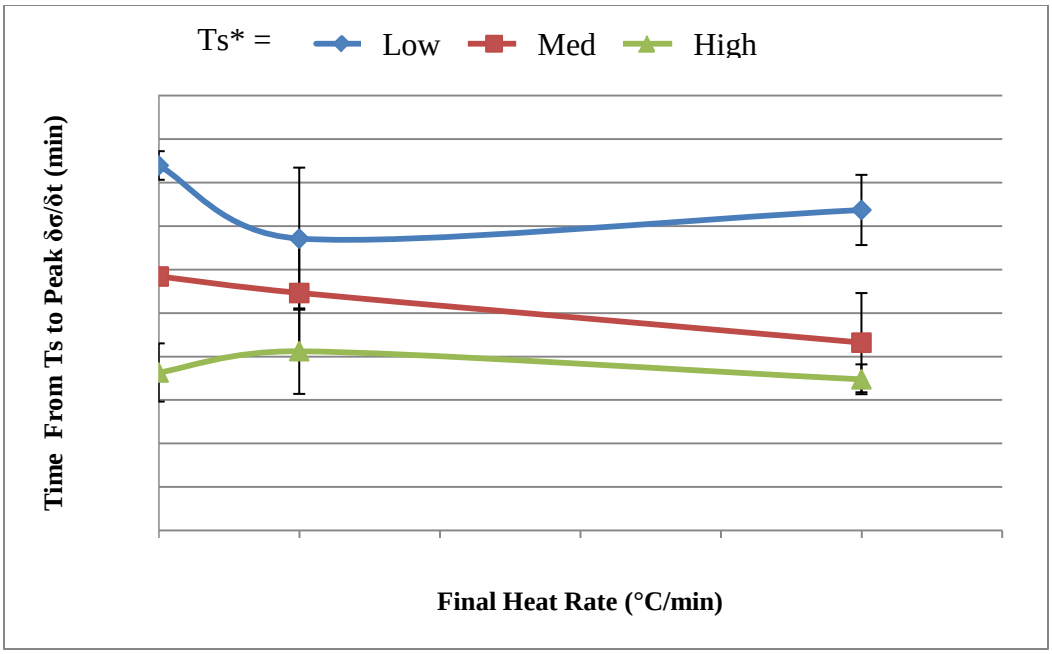

Figure 4-9: Time from T_s* to Peak δσ/δt vs Final Heat Rate (time relative to T_s*)

Observing the above figure, the data within each T_s* value can be seen to be almost entirely within error. However, there exists some separation between each T_s* value. The table below has averaged the time to peak from T_s*.

Table 4-3: Average time from T_s* to maximum δσ/δt

Ts*(°C)	Time to max δσ/δt(min)

What this table provides is another insight into the reaction kinetics of the stabilization reactions. At the higher temperatures, more progress has been made toward the activation energies of the stabilization reactions. The maximum slope of the stress can be analogous to the exothermic peak in DSC experiments. If DSC ramps were done with the same temperature profiles as the DMA experiments in this section (including the secondary ramp after T_s*), the data in Figures 4-8 and 4-9 would likely be excellent predictors for the peak heights and exothermic peak time, respectively.

4.2.4 Results Continued – Studying DDR = 10.7

After the study of the DDR = 5.9 precursor fibers, a selection of testing parameters from the original experimental matrix in Table 4-1 were run to study how different spinning conditions may affect the stabilization procedure. Below is a table showing the matrix used to study the glycerol stretched precursor fibers.

Table 4-4: Testing Matrix for DMA Stress / Isostrain Studies of DDR = 10.7 fibers

	T_s* = Low °C	T_s* = Med °C	T_s* = High °C
Final ramp = Slow °C/min	X		X
Final ramp = Mod. °C/min	X**		
Final ramp = Fast °C/min	X		X

Three samples tested per level

**Denotes level selected for batch stabilization, carbonization, and tensile testing.

The samples were prepared and the results were analyzed in the same manner as the DDR = 5.9 fibers. The table below shows a summary of the results found through the DMA studies.

Table 4-5: Summary of the results of observed stress during stabilization in isostrain conditions

	Final Temperature Ramp
Avg Peak Stress (MPa)	
STD DEV	
Avg Time at Peak Stress (min)	
STD DEV	
Avg δσ/δt (Mpa/min)	
STD DEV	
Avg δσ/δt time (min)	
STD DEV	

The primary objective of these experiments was to create a comparison between the results in Table 4-5 and Table 4-2. First, when observing the resulting peak stress values during the same temperature profiles, Figure 4-10 shows that the higher draw ratio results

in a higher stabilization stress at peak. For the two points studied with a final heating rate of (Fast) °C/min, the values are closer together, but with more conservative final heating ramps, the more drawn fibers developed a higher peak stress.

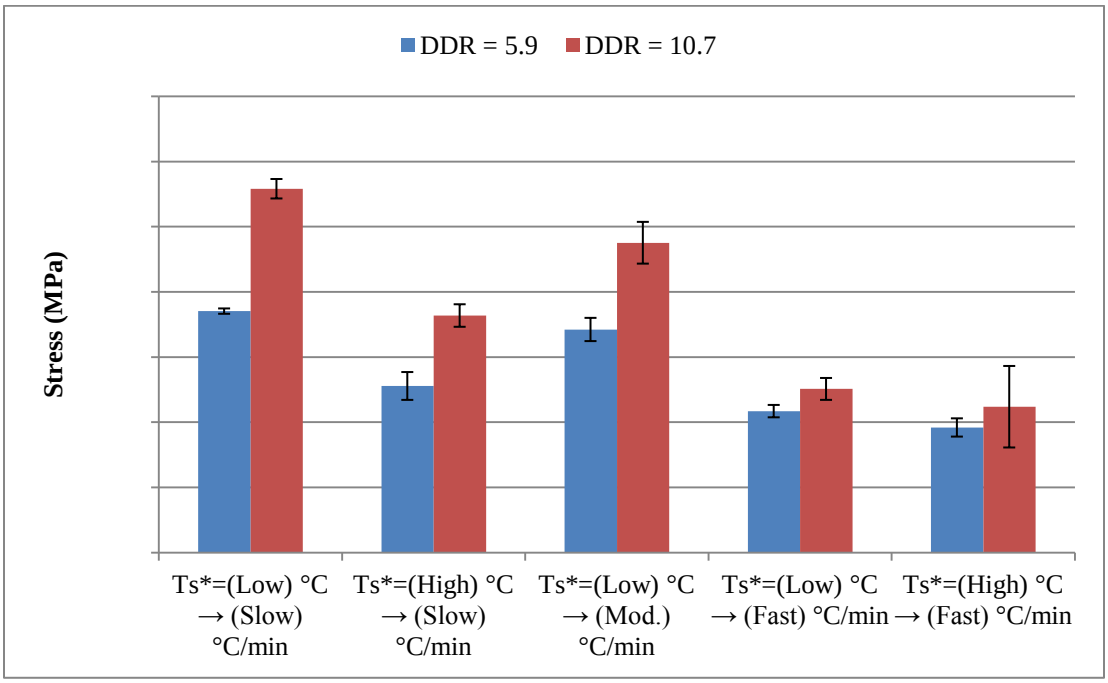

Figure 4-10: Peak Stabilization Stress between DDR = 5.9 and DDR = 10.7 precursor fibers

When comparing the two precursor draw ratios with regard to the time necessary to reach the peak stress, the values are much closer together.

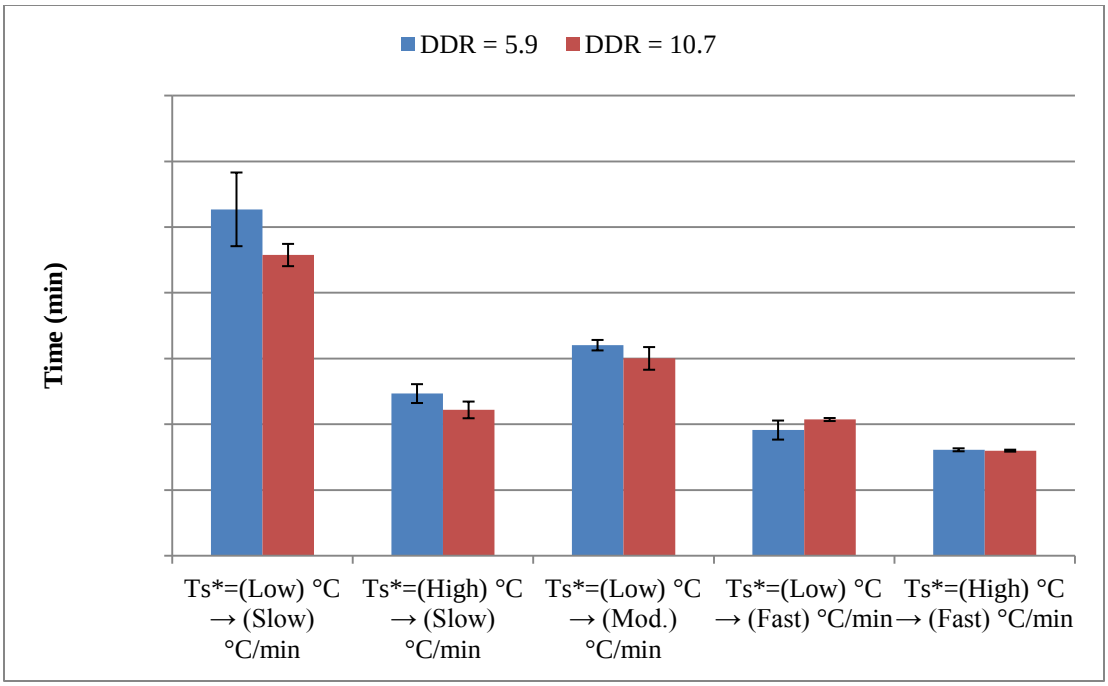

Figure 4-11: Time to peak stabilization stress between DDR = 5.9 and DDR = 10.7 precursor fibers

Lastly, the next two figures will show the peak values for the time derivative of stress, along with the time taken to reach that point after the T_s* temperature had been reached.

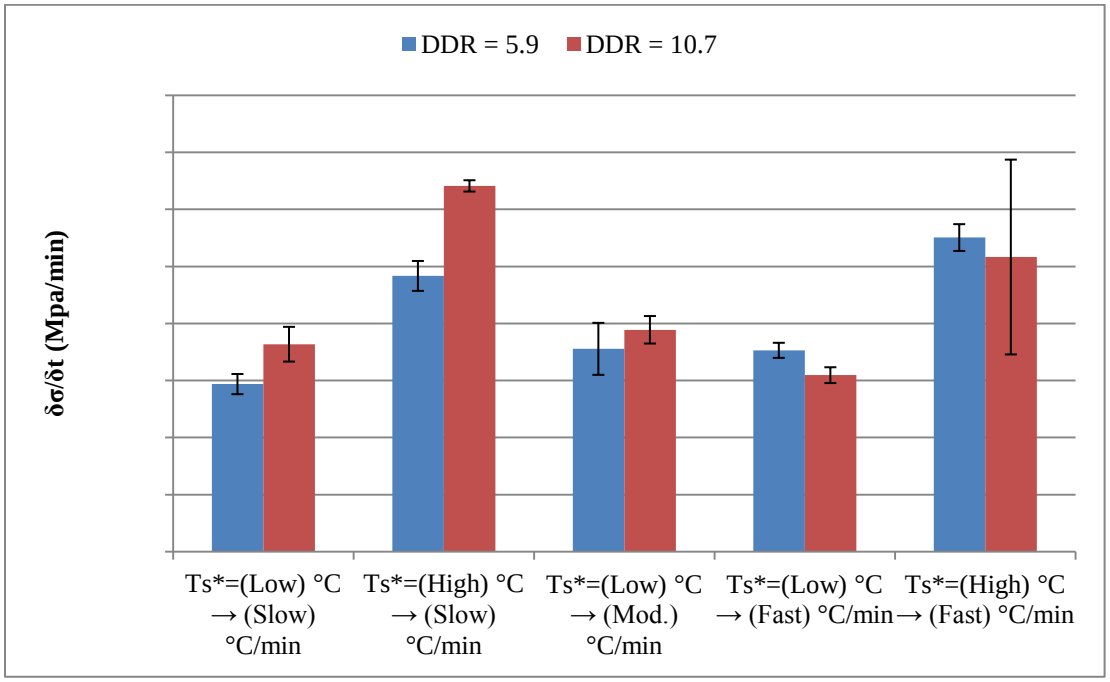

Figure 4-12: Peak δσ/δt (Mpa/min) between DDR = 5.9 and DDR = 10.7

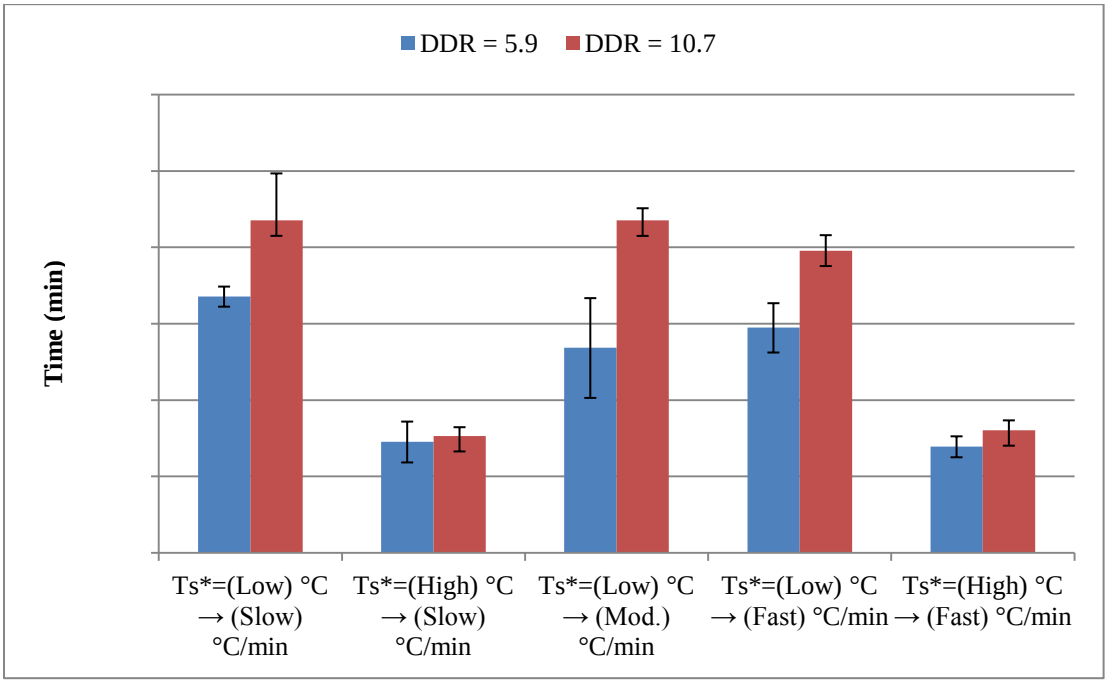

Figure 4-13: Time to peak $\delta\sigma/\delta t$ (Mpa/min)(relative to T_s*) between DDR = 5.9 and DDR = 10.7

In figures Figure 4-12 and Figure 4-13, the maximum value of the slope of the stress was recorded as in indicator for the speed that the reactions are taking place. As stress increases with the onset of stabilization reactions, the rate of that increase may be a comparative indicator. Additionally, the fastest slope of increasing stress happens within @ minutes of the selected T_s* temperature, and recording how long the max slope needed with respect to the start of the final heating rate can be an indicator for the selection of the T_s* value or the final heat rate.

4.2.5 Conclusion

A matrix of temperature profiles was studied under stress-isostrain conditions in the DMA. The intent was to develop a relationship between the temperature profile and the stress profile of the fibers during stabilization. With this study, continued research into the relationship between the *in situ* stress and properties can be made, so that ultimately, an optimized temperature profile can be developed for the precursor fibers.

The temperature profile that attained the highest peak stress in the stabilizing fibers occurred with the most conservative temperature profile of T_s* = (Low) °C followed by (Slow) °C/min conditions. This implied that the scope of the experimental matrix can be expanded to lower temperatures to find where the trend continues. At lower T_s* values the max stress may even reach higher numbers as implied in Figure 4-6. The question is how low can T_s* go until the time needed to reach the max stress and fully stabilize becomes inordinately too long? The profile that achieved the highest stress also came with the longest residence time. Additionally, too low of a T_s* value will fail to take the fibers beyond the activation energy, and not even initiate the stabilization reactions.

At this point, bridging the gap between temperature profile and the stress profile does not provide any insight if the values for peak stress are any indicator for carbon fiber quality. However, some observations can be made about the general profiles of the stress curves versus time, and they can perhaps be used to determine when the fibers are fully stabilized. With the works of others proposing that the lessening of shrinkage in a TMA can indicate the slowing of stabilization reactions [54] to the transition times to storage and loss modulus values in a DMA indicating the cessation of reactions[66], the transition time for stress may also be a valid indicator. The preferred characteristic of the test in this work is that it holds the fiber in isostrain, where the TMA allows shrinkage and obtaining storage and loss modulus values must allow for length changes. This is important since the fibers that will be batch stabilized in this work will be done in isostrain conditions, and fibers that are stabilized continuously will not allow for shrinkage.

Looking closer at some examples of stress profiles, in particular in Figure 4-4, it can be seen that the second heating ramp rate of (Fast) °C/min resulted in an early stress peak that was much lower than the others and sharply fell after the peak. It can be assumed that this choice of heating ramp was not optimal, even if the stress value is not an indicator of quality, the sharp decrease may indicate fiber damage or even melting from the exothermic reaction. The more conservative temperature profiles did not have such a

significant drop, which shows that those ramps were appropriate for the quick reactions of this homopolymer PAN.

Finally, a study comparing five of the nine temperature profiles was performed with the precursor fibers that were glycerol stretched (DDR = 10.7). Those fibers saw an across the board increase of *in situ* stress during stabilization, along with higher peak stress values. The argument can be made that the reduction of diameter, and further molecular alignment during the additional stretching, contributed to the higher stress. The times that were needed to obtain the peak stress values were also slightly reduced, or stayed within error. This is most likely due to the reduced precursor diameter allowing for improved mass and energy transfer into the fibers due to the higher surface area to volume ratio. Additionally, the rates of stress increases were higher in the DDR = 10.7 fibers, which shows that the cyclization reactions proceeded at an increased rate. And the results show that the glycerol stretched fibers took longer to reach their respective maximum slopes of stress increase. Recall the results and conclusions from the DSC studies of the glycerol stretched fiber. The fibers with the higher draw ratio had a higher activation energy. The stress profile increasing slightly later and stronger in the DMA, reinforces the conclusion that the precursor macro-molecular structure developed a more oriented and crystalline structure. As stabilization reactions are initiated in the amorphous regions, a reduction in amorphous PAN chains would delay the increase of stress. But with ultimately higher slopes being seen, it is shown that the cyclization reactions are reaching the more populous crystalline regions.

4.3 Optimizing the Temperature Profile – Linking *in situ* Stress to Final Properties

4.3.1 Introduction

After building a relationship between the temperature profile and the stress development of the stabilizing fibers, some of the parameters were used for batch stabilization of the precursor fibers, then carbonized under identical conditions, and tested for the final carbon fiber properties. By testing the final carbon fiber properties, a relationship between the stabilization procedure and the ultimate properties may be produced, completing the link between the DMA experiments and the carbon fiber properties. The

conclusions of Section 4.2 were that the values of the peak stresses in the DMA may or may not be an indicator of final carbon fiber tensile properties, but that will be tested in this section. Additionally, the hypothesis that the time to peak stress was an indicator for completion of stabilization reactions will be tested by using those times for the batch stabilization procedures.

4.3.2 Method and Equipment

The 100 count tow precursor fibers were spun onto spools with a traversing winder. The process to stabilize and carbonize the precursor fibers was done by taking a small amount of fiber to create a "hoop tow." This is done by unwinding a length of precursor from the original spool onto another spool with little to no traversing of the fiber. The fiber tow will then overlap on itself, and the effect of entanglement and friction will keep the tow in a "hoop" when removed from the spool without any need for a knot in the fibers.

The hoop tow of fibers was then mounted onto a stainless steel rack to maintain isostrain conditions during stabilization. Pretension was not measured, but the rack was tightened such that when pressure was applied manually to the middle of the tow (between the two steel rods), there was little bow in the fibers. This was to reduce if not eliminate any fiber shrinkage that could occur during stabilization. Concerning pretension, any variability was assumed to have a negligible effect on the final outcome of the fibers, as it has been shown that differing levels of pretension result in little tension change after the glass transition temperature [7].

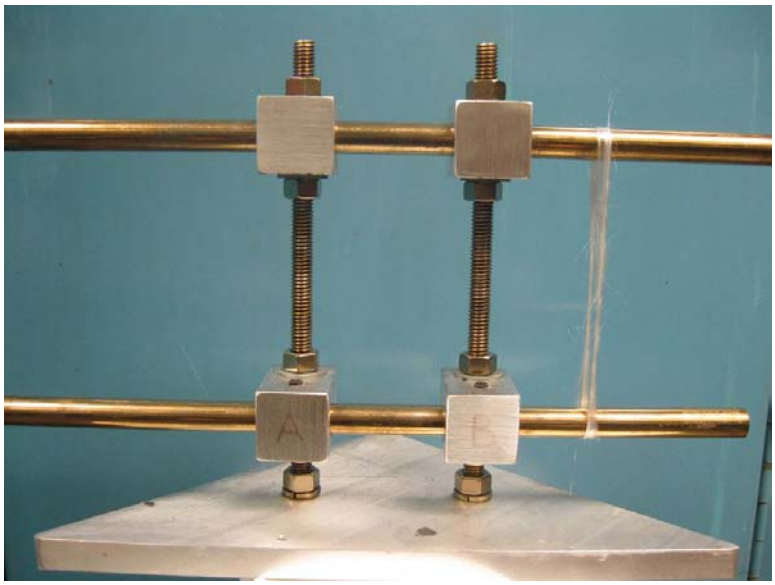

Figure 4-14: Stainless Steel Isostrain Stabilization Rack

The rack is then placed in a furnace and programmed to run along one of the stabilization paths from the DMA experiments, as shown in Table 4-1 and Table 4-4. A data logger was used to record the process temperature within the oven, to ensure that the profile followed the parameters. Two thermocouples were placed within the oven, approximately 2-3 inches on either side of the hoop tow. During the runs, the oven maintained temperatures within 2-3 °C of the desired process temperature.

The DDR = 5.9 fibers were stabilized under two separate parameters. The first, T_s* = (Low) °C with a final ramp of (Moderate) °C/min, and the other being T_s* = (High) °C with a final ramp of (Moderate) °C/min. These were selected because the former was mentioned earlier as a result with a high *in situ* stress within a shorter time to peak stress (it was the second highest stress, after the T_s*= (Low) - (Slow) profile). The latter was a representative profile that modified only one of the two temperature parameters, yet lowered the peak stress drastically. (To recall, the first temperature profile had a peak stress of @ MPa and the second was @ MPa.) Additionally, one hoop tow of the DDR = 10.7 precursor fibers was stabilized under the same conditions as the one above (T_s* = (Low) °C with a final ramp of (Moderate) °C/min) to observe the effects of different spinning conditions on the final properties.

The batch stabilization furnace was run under those two profiles, and when the oven reached the temperature and time where the max stress was recorded in the DMA studies, the rack assembly was promptly removed from the furnace to cool to room temperature. Once cooled, the mass of the fibers were recorded and they were then prepared for carbonization.

Unlike the batch process of stabilization, where the fibers were held in isostrain conditions, batch carbonization was done with a constant tension method. A hoop tow of fibers was mounted in a graphite rack with a hanging mass to maintain tension. The rack can accommodate several configurations of hanging masses to increase pressure, but since only ten revolutions of 100 count tow were used to make the hoop, a lighter load was selected. The diameters of the fibers after stabilization were not measured, but if they were to remain close to the original precursor diameter, the mass of the graphite block and the assumed area can produce an estimate for the tension endured by the fibers.

$$Pressure = \frac{\left(9.81\frac{m}{s^2}\right)(@\ kg)}{\left(460.13\ \frac{micron^2}{fiber}\right)(2000\ fibers)\left(10^{-12}\ \frac{meter^2}{micron^2}\right)} = 110\ kPa$$

To demonstrate the hanging block method used in the graphite furnace, observe Figure 4-15.

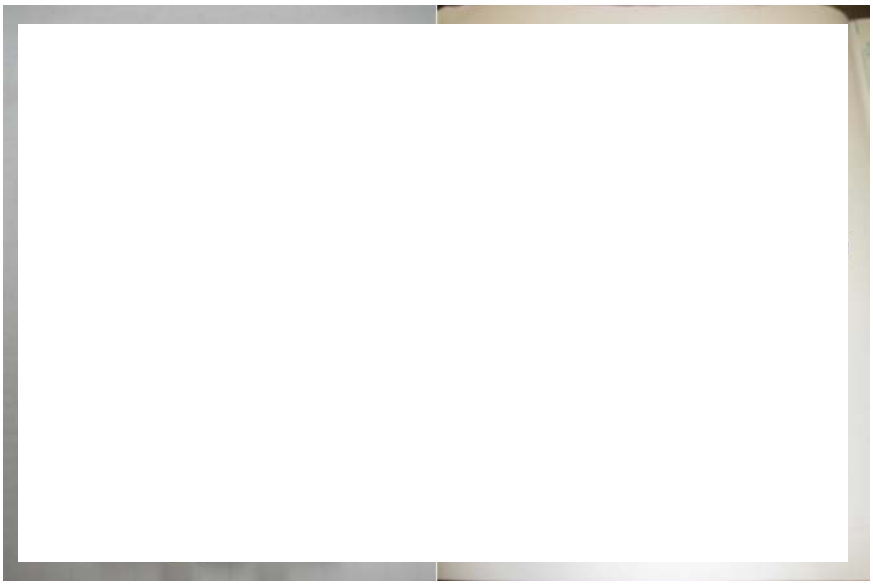

Figure 4-15: Left: Stabilized hoop tow mounted to hanging rack with one block; Right: Rack hanging in graphite crucible

All fibers were carbonized with the same procedure. @ °C/min to @ °C, @ dwell, then @ °C/min back to room temperature. The selection of procedure was selected due to prior experience with carbon fiber carbonization, but it is also backed in literature. Going any higher than 1300-1500 °C can result in pitting and deformities of the fiber due to the volatilization of foreign particles[49, 54]. As for heating rate, Fitzer's work demonstrated through a selection of carbonization rates that high ramps (approximately 50 °C/min and above) cause a decrease in the tensile strength of the resulting carbon fibers. This was suggested to be attributed to increased rate of carbonization reactions and mass diffusion causing damage to the fibers. Inversely, too slow a rate also decreased the strength, which was thought to be due to a longer residence time in a furnace chamber that may have had lingering oxygen in the crucible [54].

Tensile tests were performed on an MTS Systems Q-10 measuring device. In use was a 150 gram load cell. For each batch of carbonized fiber, 120 aperture cards were mounted with a single filament of carbon fiber. Because of the soft load cell, the 120 aperture cards varied in gauge length in order to calculate system compliance. A quantity of 4 different gauge lengths were represented, resulting in 30 aperture cards of 20 mm, 30 mm, 40 mm, and 50 mm in gauge length. Each fiber was mounted with a small

application of glue at the inside edge of the card opening. Once mounted, the cards were cut at an angle and bent or removed so that they do not interfere with testing.

Figure 4-16: Left: Aperture card mounted to clamps; Right: Card cut, sample ready to test

Testing parameters were contingent with ASTM 3379-75. The fibers were tested such that each specimen took approximately one minute from application of load to breakage. For these fibers, 0.2 mm/min was the chosen speed for the crosshead movement.

4.3.3 Results

DDR = 5.9 fibers were studied at T_s* = (Low) °C with a (Moderate) °C/min final heating ramp, and the same was done with the batch of DDR = 10.7 fibers, to compare between the two precursors. Additionally, another batch of DDR = 5.9 fibers were stabilized at the T_s* = (High) °C and h_f = (Moderate) °C/min, in order to compare between one modification to the stabilization procedure that resulted in a much lower peak stress as shown in DMA studies. For simplicity, these fibers will no longer be referenced by their spinning and stabilization parameters, but rather will be denoted A, B, and C. Observe Table 4-6 for the naming convention.

Mass changes were recorded before and after stabilization, and mass and length changes were recorded before and after carbonization. Summarized in Table 4-6, the stabilization

profile for fibers A resulted in the highest mass yield during stabilization and carbonization. This may be an early indicator that the procedure used was the most thorough and that the fibers were stabilized to completion. Shrinkage values under the same force were quite close. Notable, is that the fibers with the higher spin draw ratio, were carbonized under the highest pressure due to the reduced cross sectional area, yet experienced similar shrinkage to the others.

Table 4-6: Mass and length changes during stabilization and carbonization

		Stabilization			Carbonization			
Carbon Fiber	Fiber DDR	Ts* (°C)	h-f (°C/min)	Mass Yield	HTT (°C)	h-carb (°C/min)	Mass Yield**	Shrinkage
A	5.9	Low	Moderate	95.6%			51.3%	10.8%
B	5.9	High	Moderate	91.4%			48.8%	10.1%
C	10.7	Low	Moderate	89.1%			49.4%	11.0%

** relative to precursor mass

A sample of each hoop tow was then studied with a scanning electron microscope (SEM) for diameter measurement. As expected, the diameter of the two fibers spun under DDR = 5.9 conditions had similar final diameters, and the glycerol stretched fibers were smaller after stabilization and carbonization. Of note, however, is that the standard deviation of those diameter measurements for the DDR = 10.7 fibers is at least double compared to the other fibers. The diameter and circularity values from the original precursors were included for reference in Table 4-7 below. The primary difference between Fibers A and C is the glycerol stretching. This would lead to the conclusion that the glycerol stretching caused anomalies or was inconsistent throughout the length of fiber. However, that hypothesis is rebutted by the superior standard deviation of the precursor fiber measurements, where the larger deviation occurs after the process of stabilization and carbonization. It is important to note, that the samples collected for measurement were at different lengths of the collected fiber tow. It is possible that the glycerol stretching damaged or inconsistently stretched fibers within the tow, and defects simply were more prevalent in the portion used for batch stabilization and carbonization.

Table 4-7: Carbon fiber diameter and circularity measurements

Carbon Fiber	Precursor			Carbon Fiber			
	Diameter (micron)	Circularity	# Samples	Diameter (micron)	Circularity	# Samples	
A	24.15	0.56	31	13.42	0.49	33	Average
	1.65	0.03		1.15	0.02		STD DEV
B	24.15	0.56	31	13.46	0.46	31	
	1.65	0.03		0.80	0.01		
C	20.60	0.56	38	12.80	0.49	37	
	1.57	0.02		2.30	0.08		

Tensile properties, including break stress and tensile modulus, were found by single filament testing. Observing Table 4-8, Fiber A, stabilized under the higher stress parameters relative to Fiber B, saw the same tensile stress and slightly higher modulus. These values are not directly proportional to the peak stress from stabilization as observed in the DMA studies, as the values are significantly within error. Furthermore, Fibers C, which were glycerol stretched but otherwise treated identically to Fibers A, experienced a higher *in situ* stabilization stress, but suffered a significant drop in ultimate carbon fiber tensile properties, yet maintained similar modulus values.

Table 4-8: Summary of carbon fiber tensile properties

Carbon Fiber	Stabilization Procedure			Final Carbon Fiber Tensile Properties					
	Spinning DDR	Ts* (°C)	h-f (°C/min)	Diameter (micron)	Stress At Break (MPA)	Modulus (GPa)	Strain At Break (%)	Strain Energy Density (MJ/m³)	
A	5.9	Low	Moderate	13.42	1594.960	230.07	0.69%	5.87	Average
				1.15	463.763	26.79	0.17%	2.87	STD DEV
B	5.9	High	Moderate	13.46	1523.908	203.12	0.75%	6.11	
				0.80	443.069	18.92	0.20%	2.90	
C	10.7	Low	Moderate	12.80	1048.651	228.21	0.46%	2.60	
				2.30	346.370	31.33	0.13%	1.36	

The final stress-at-break numbers were fitted for probability to failure analysis using a Weibull distribution. The general form for the Weibull distribution used is:

$$F(\sigma) = 1 - exp\left[-\left(\frac{\sigma}{\sigma_0}\right)^m\right]$$

Where F function is the probability to failure, σ is the applied stress in MPa, σ_0 is the scaling parameter, and m is the shape parameter. The scaling parameter and shape parameter are found by linearization of the function into the form:

$$ln\left[ln\left(\frac{1}{1-F}\right)\right] = m * \ln(\sigma) - m * \ln(\sigma_0)$$

In summary, the parameters for the Weibull distributions for each of the three fibers are as follows, along with the probability to failure plots.

Table 4-9: Shape and scale parameters for Weibull analysis

Carbon Fiber	m	σ-o	R^2
A	3.6640	1770.10	0.99
B	3.3747	1704.74	0.98
C	3.0309	1179.31	0.98

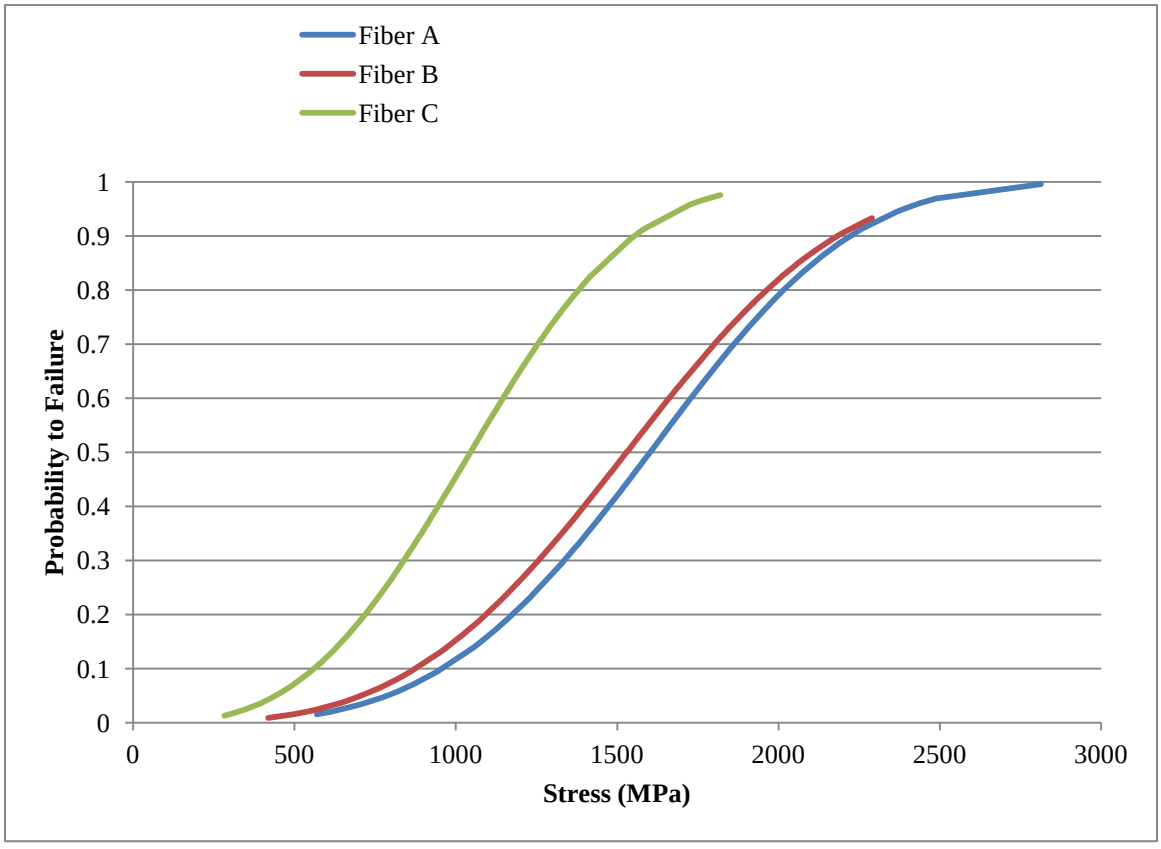

Figure 4-17: Probability to failure for carbon fibers A – C

The shape parameter (m) is largest with Fiber A, and is seen to flatten out the curve over the largest region of stress values. Oppositely, Fibers C have the smallest shape parameter values and have a slightly more vertical trend line. This is analogous to the standard deviation for tensile strength in Table 4-8 The scale parameter is close between Fibers A and B, but A is slightly higher, which corresponds to the overall location on the x-axis. Fibers C have a much lower value, which is evident by the offset to the left, relative to the other two values. The scale parameter is related to the overall strength.

4.3.4 Conclusion

Although not an extensive study among all the levels observed in Section 4.2, differing stabilization and precursor conditions were studied by batch stabilization, carbonization, and tensile testing. Fiber A, was the "high peak stress" option from the DDR = 5.9 precursor fiber, where Fiber B was the "low peak stress" option from the same precursor. The only difference between the two was their selected T_s* temperatures for the stabilization temperature profile. And as a result, the averages of the ultimate carbon fiber break stress shows Fiber A slightly greater than Fiber B, but the two are very much within their error bars. This shows that the values for peak stress found in the DMA experiments is not an indicator for the final carbon fiber tensile strength, but possibly for the tensile modulus.

When comparing the two different spinning stretch ratios that had identical stabilization and carbonization conditions, Fibers A and Fibers C, the two different peak stress values during stabilization resulted in the opposite results for the carbon fiber tensile properties. This further shows the lack of correlation between peak stress during stabilization and the final carbon fiber tensile properties. However, it should be noted that the glycerol stretched fibers may have been compromised in the act of stretching, and perhaps should not be considered when making conclusions on the relationship between peak stabilization stress and carbon fiber tensile stress.

4.4 Conclusion

This chapter sought to make a connection between stabilization temperature profiles and the resulting carbon fiber properties through the use of DMA studies observing stress in

isostrain conditions. A strong relationship was built between the temperature profile and the *in situ* stress, but the points of comparison selected for batch stabilization and carbonization did not show a correlation between peak stress and final tensile properties. The two methods used between the same precursor, showed marginal difference, though the higher stress profile resulted in higher carbon yield and slightly raised the average tensile properties, generously within error. Comparing two differing spinning stretch parameters with similar heat treatment showed an inverse correlation between stress and the final properties. The DDR = 10.7 fibers had a substantially higher stabilization stress and significantly lower carbon fiber break stress. In summary, the value for the peak stress during stabilization bears no predictive value on the ultimate carbon fiber properties with these fibers.

The issue of complete stabilization may be raised for the given temperature profiles. Observing when the *in situ* stress leveled off and peaked was used as the finishing time for stabilization. The strong increase in stress is believed to be attributed to the cyclization reaction, and the slow increase in stress is for the continuing reactions of dehydrogenation (due to the work done in section 5.2). For Fiber A, time associated with the peak stress was @ min after T_s*, for Fiber B, @ mins, and for Fiber C, @ min. When comparing to the stabilization method used before the work in this thesis, the final carbon fiber properties are shown to not be much different. However, the time taken for stabilization has been significantly reduced to achieve the same ultimate properties. The residence time used in the "old" method was @ mins. With savings of anywhere to @ to @ in the post T_s* time alone, the same carbon fiber properties have been achieved. For a demonstration, the Weibull plot of one set of precursor fibers spun under the same conditions, stabilized under the "old" method, and carbonized in the same manner, is much in line with the results from this work.

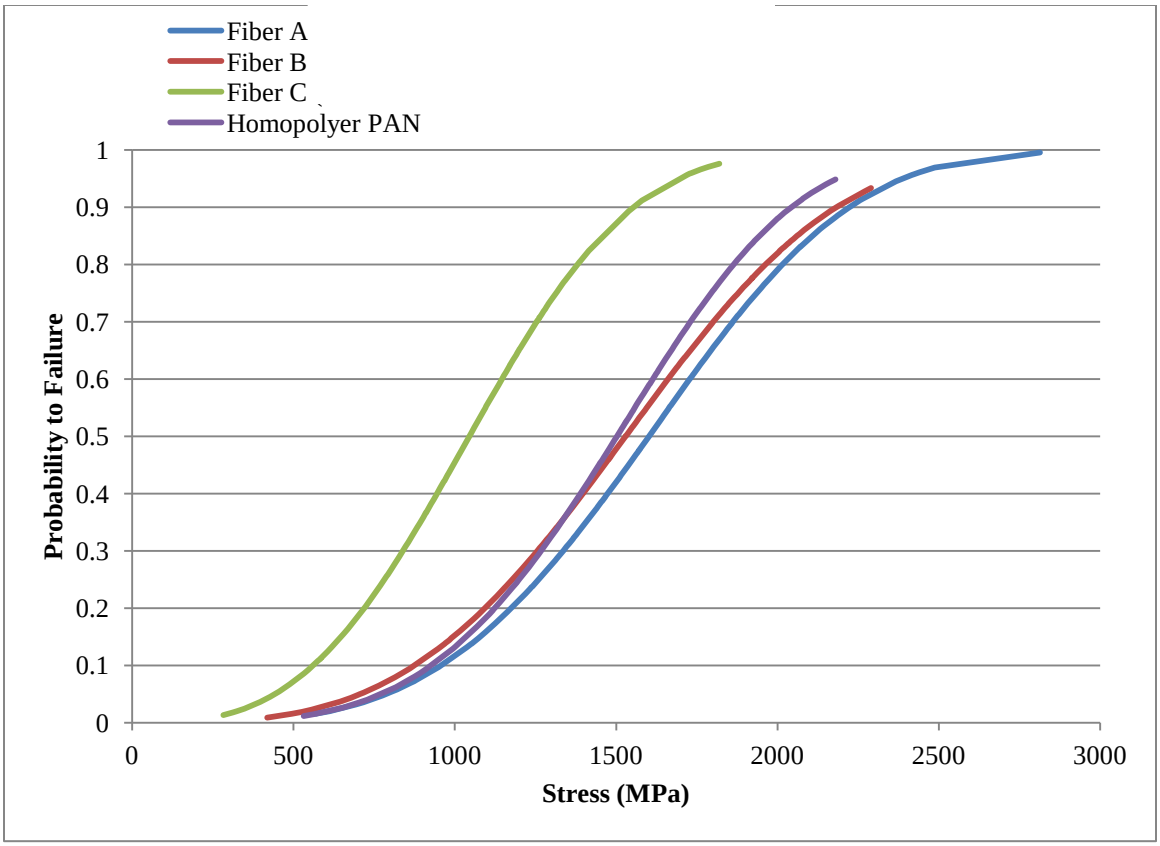

Figure 4-18: Probability to failure of the carbon fibers in this work compared to similar spinning conditions but stabilized with the "old" method

It can be seen in Figure 4-18 that the stabilization procedures for Fibers A, B, and the fibers stabilized with the old method are very similar in their ultimate tensile strength characteristics. With identical dope formulation and spinning conditions, the “old” procedure was stabilized at @ °C for @ hours, after a @ hour ramp to that temperature. Those fibers were certainly allowed ample time to fully stabilize. Regardless, the same tensile properties were achieved through stabilization procedures lasting around @% of that time. But carbon fiber tensile strength is not the only factor under consideration. Young’s modulus has also been recorded, and Table 4-10 demonstrates that the shortened stabilization treatment did not hinder the modulus values. With the final properties being held constant, when compared to a heat treatment that is very conservative, it can be concluded that the procedures used (and the rubric of following stabilization to the peak stress during isostrain conditions) may be a useful tool in assuming that the stabilization reactions have adequately been completed.

Table 4-10: Summary of carbon fiber tensile properties including parameters used before this work

Carbon Fiber	Stabilization Procedure				Final Carbon Fiber Tensile Properties					
	Spinning DDR	Ts (°C)	h-f (°C/min)	Peak Stress MPa	Diameter (micron)	Stress At Break (MPA)	Modulus (GPa)	Strain At Break (%)	Strain Energy Density (MJ/m³)	
A	5.9	Low	Moderate		13.42	1594.960	230.07	0.69%	5.87	Average
					1.15	463.763	26.79	0.17%	2.87	STD DEV
B	5.9	High	Moderate		13.46	1523.908	203.12	0.75%	6.11	
					0.80	443.069	18.92	0.20%	2.90	
C	10.7	Low	Moderate		12.80	1048.651	228.21	0.46%	2.60	
					2.30	346.370	31.33	0.13%	1.36	
"Old"	5.9	Lowest	Slow		13.78	1479.424	220.04	0.67%	5.11	
					1.14	380.218	41.18	0.11%	1.85	

Lastly, Fiber C is an outlier in the final carbon fiber results. In previous studies, over-drawing of the fibers after the glass transition temperature before stabilization has been found to result in plastic and elastic deformation (or slippage) of the amorphous and crystalline regions of the precursor fiber, resulting in diminished carbon fiber properties[44]. Though only one stretch ratio has been performed, a draw ratio of 1.8 within the compliant temperature region may have been too aggressive for the given precursor. Stretching in air with the same precursor fiber resulted in breakage below @% (Ch. 5 of this work), which is difficult to relate to stretching in glycerol. (The glycerol stretching done with a draw ratio of 1.8 for Fibers C equates to a strain of 45%.) Though glycerol stretching may have a potentially higher maximum potential for stretching, it can only be assumed based on the final carbon fiber properties that the fibers used in this work were stretched to the point of damaging the structure of the fiber, thus inhibiting its tensile properties. Further studies with an array of smaller draw ratios would provide a clearer spectrum of possibly ideal draw ratios.

5 STATE OF REACTION DURING STABILIZATION: OPTIMIZATION OF THE STRAIN PROFILE

5.1 Introduction

Strain imparted to stabilizing fibers is one of the major contributors to providing optimized carbon fiber properties. Strain increases molecular alignment, defects can be reduced, and overall tensile strength and modulus improvements can be seen. Optimizing the temperature profile for stabilization of precursor fibers without strain is already a complex task, and adding a strain profile produces more complexities for understanding how to produce optimized carbon fiber properties.

It has been shown that adding strain can affect the optimized temperature profile [66]. Stretching the fiber would reduce the overall cross-sectional area, aiding the energy and mass diffusion processes needed for stabilization. Therefore, the optimized time under temperature when the fiber has been stretched would be reduced. In this section, however, the effect of stabilization strain on the ultimate carbon fiber properties was not studied. Nonetheless, a more rudimentary study was performed to gain a general understanding of strain during stabilization, to answer the questions of when in the stabilization procedure is it best to apply strain, and by how much strain.

5.2 *In Situ* Stress vs. Strain Analysis in Isostrain Stabilization

5.2.1 Introduction

A set of experiments were performed in order to study the maximum amount of strain that fibers can endure throughout the process of stabilization. This set of experiments was done before the work performed in Chapter 4, and therefore, does not resemble the same temperature profiles seen in any other part of this work. However, it is a useful study for identifying the time and temperatures during stabilization which offer the greatest amounts of allowable strain to stabilizing fibers, and it provides insight into the previous method of stabilization used before this work that was also mentioned in Chapter 4.

5.2.2 Method and Equipment

Performed on a TA Instruments Q800 series DMA, the sample preparation and mounting was very similar to the procedure done in section 4.2.2. One hundred filament count tows of the DDR = 5.9 precursor fibers were mounted to aperture cards, but the exception with these experiments was that the fibers were not secured to the aperture cards with epoxy, but rather with polyimide adhesive tape. (The epoxy method was used to alleviate the occurrence of early breakages at the clamp during the reaction exotherm, which was not a problem using a conservative temperature profile.)

The temperature profile also deviated from the "ramps" used in previous sections of this work. In this set of experiments, the temperature profile took on a more stepwise profile.

Table 5-1: Time and Stepwise Temperature profile for Experiment

Zone	
Temperature (°C)	
Time from Start (min)	

Zone	
Temperature (°C)	
Time from Start (min)	

Samples were taken through the temperature profile in isostrain conditions in the DMA, similar to section 4.2. Additionally, not every sample was taken to the end of the temperature profile. At certain time and temperatures, a point of observation was made during experimentation. Some samples were taken to each point, where the procedure ceased and a stress to failure vs. strain test was performed at that temperature. Strain rates for the tests were varied between 0.25 %/min to 0.5 %/min, so that each stress vs. strain test lasted generally between three and eight minutes.

5.2.3 Results

Up to the points where the final stress vs. strain curves were made, *in situ* stress was recorded. For each point along the line where stress vs. strain curves were made, at least two samples were run. The stress values were taken from all the experiments, and

averaged. Below is a representation of the state of stress of the stabilizing fibers after the stress vs. strain tests were removed.

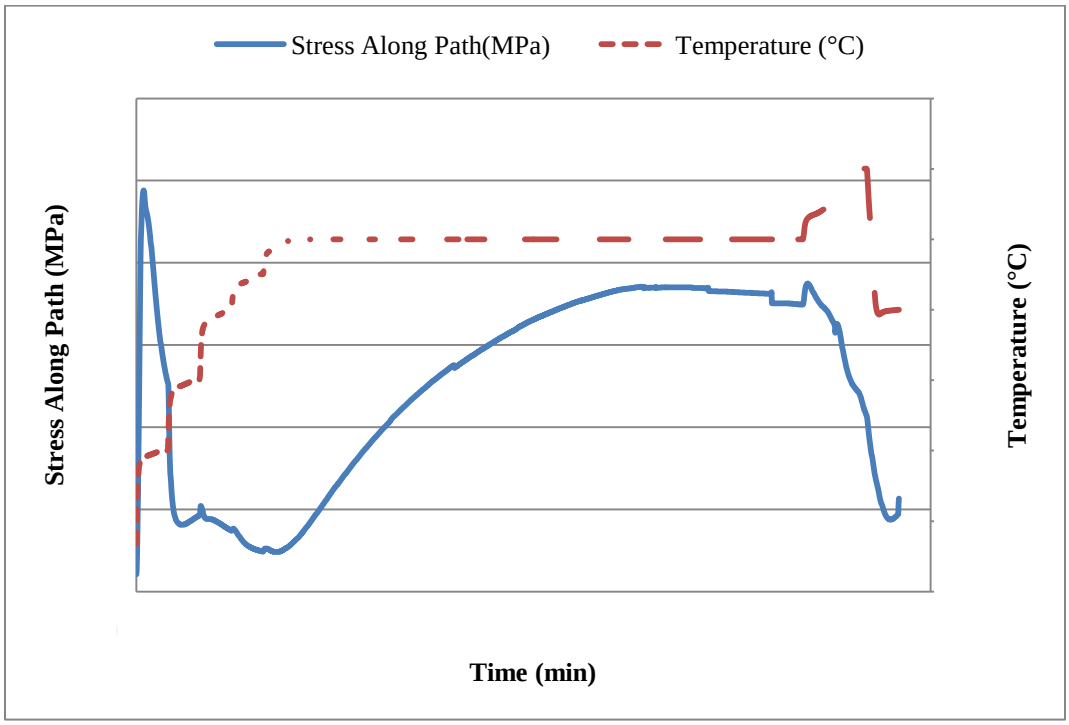

Figure 5-1: Stress vs. Time During Stabilization

Of note is that as the stress progresses with time, it follows a similar profile as the experiments done in section 4.2. A point of comparison includes the peak for the initial stress before the glass transition temperature; it is steeper and higher relative to the tests involving a smooth temperature ramp. This is thought to be a factor of the steep temperature jumps used in substitution of the smooth ramp. Also noting the latter half of the profile, the "notches" in the data that exist apart from any temperature jumps are artifacts of the averaging of multiple data sets. As fewer specimens made it to the very end of the temperature profile, losing a few specimens with 4-6 remaining has a more significant effect as opposed to losing a few specimens among dozens.

Concentrating on the data taken during the stress strain curves along the stabilization path reveals the mechanical characteristics to failure. Note the data taken in Table 5-2, Figure 5-2, and Figure 5-3 represent the data taken immediately after the isostrain-stress data has

ceased and the applied strain began. The fibers were considered broken at the first sign of any fibers being broken, not when the entire tow was destroyed.

Table 5-2: Stress and Strain at First Breakage, and Young's Modulus

Temperature (°C)	Stress at Break (MPa)	Strain at Break (%)	Young's Modulus (GPa)

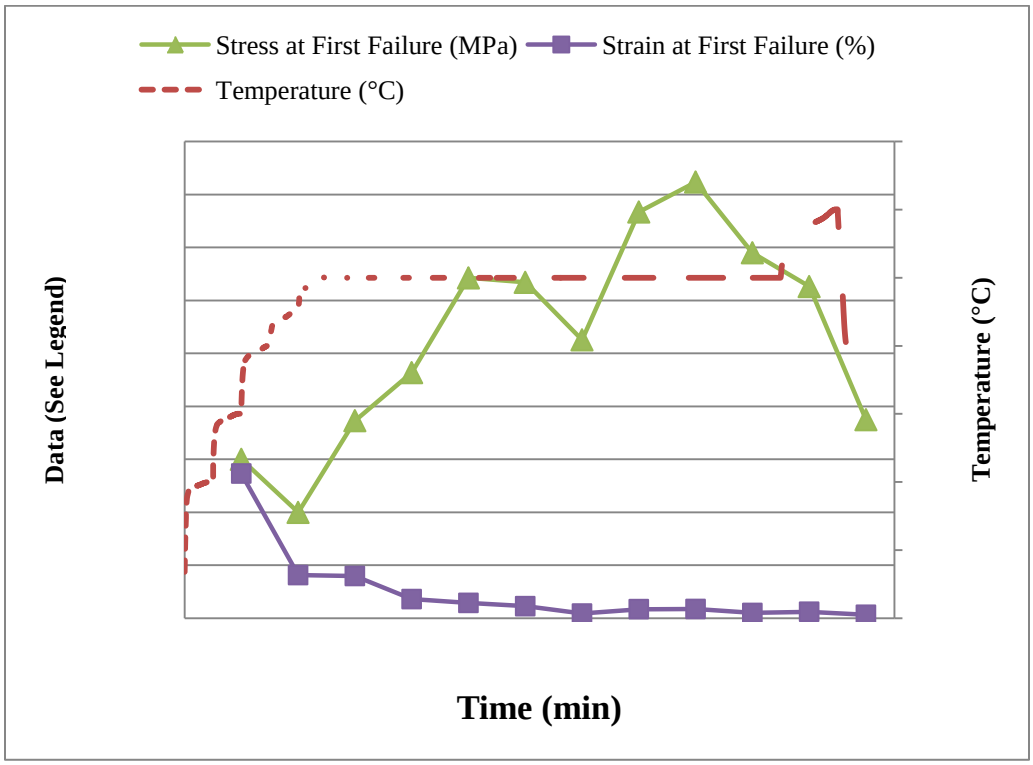

Figure 5-2: Stress and Strain at First Breakage

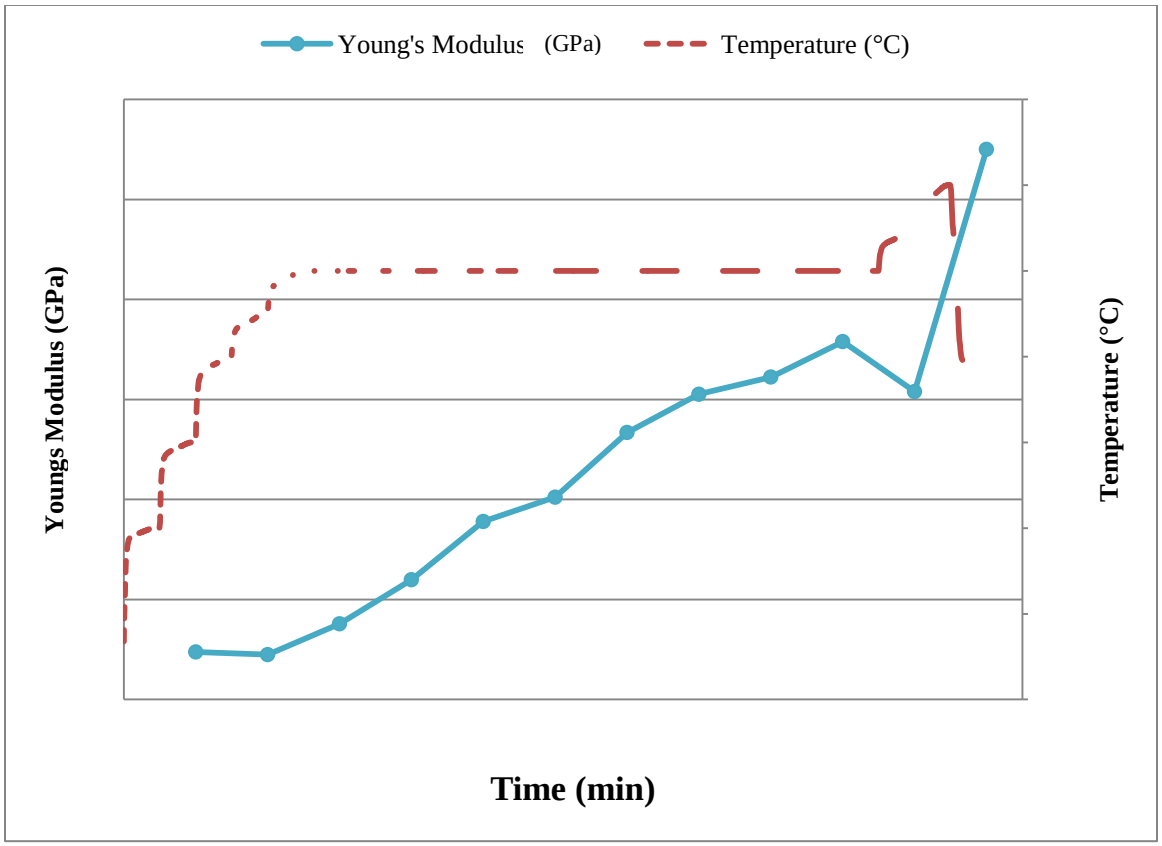

Figure 5-3: Young's Modulus during Stabilization

The above figures demonstrate that max allowable strain is highest just after the glass transition temperature and before the onset to reactions. The stress necessary for breakage generally increases with the stabilization reactions, and the Young's modulus is continuously increasing throughout the entire heat treatment.

In order to obtain further insight into the reactions occurring during this temperature profile, a DSC study was performed to follow this exact same temperature profile. Sample preparation was identical to previous DSC studies in this work (section 3.3). The DSC thermogram shows a reaction exotherm about @ minutes into the temperature dwell at @ °C. About halfway through the dwell, the peak has since flattened. Near the end of the procedure, the final exothermic peak can be attributed to further cross-linking reactions in response to the higher heat treatment.

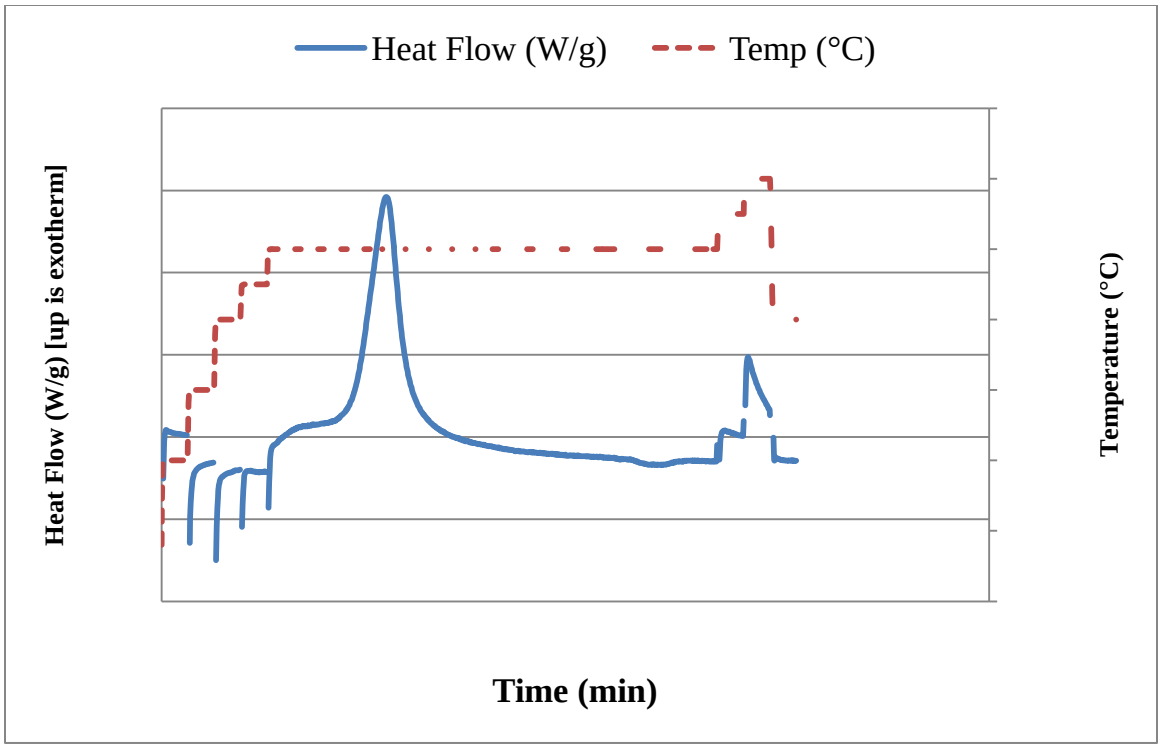

Figure 5-4: DSC thermogram following the same temperature path as the DMA experiments (note: data points corresponding with the rapid temperature jumps were removed)

5.2.4 Conclusion

It can be observed that the stress to first failure has a general trend, with some variances. During the @ °C dwell temperature, stress is steadily increasing, with the exception of the dip it takes halfway through the dwell. To ensure that the stress at breakage is not an artifact of the higher *in situ* stress, the initial stress was subtracted from the stress at breakage. This is shown below as "delta stress" in Figure 5-5 below. Even when normalized so that each stress vs. strain test started at "zero," the delta stress plot shows that the stress needed for fiber breakage was generally increasing (exception being the low point at time = @ mins). That isolated drop in stress to failure is thought to be a product of a smaller sample size, as that point in the table is the average of just two samples. More testing may show that the dip is an anomaly as opposed to a product of the fibers or stabilization procedure.

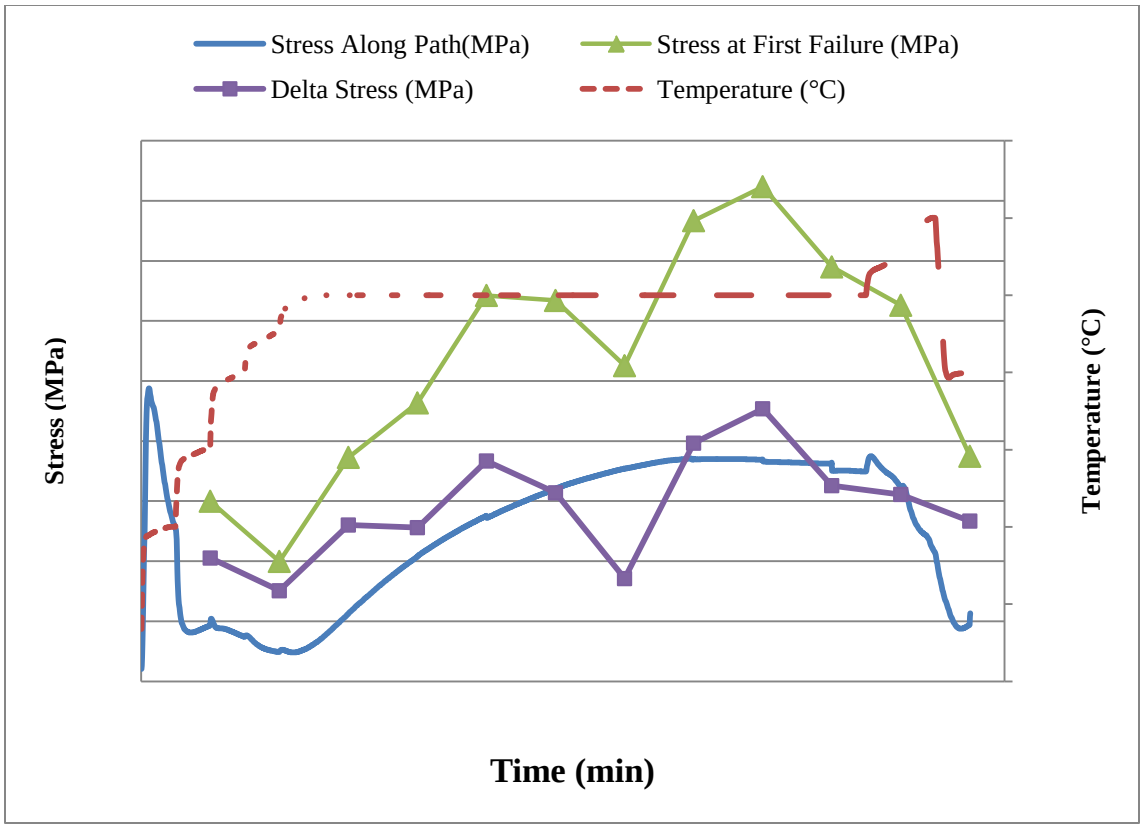

Figure 5-5: Stress during Stabilization, along with stress to first breakage and the difference between the two

The Young's Modulus that was calculated from the stress vs. strain curves shows the fiber getting progressively stiffer with heat treatment. This would most likely be a product of the continued stabilization in air allowing for continued oxygen uptake, furthering the reactions of dehydrogenation and additional oxidation. This can also be confirmed with the DSC profile, as the exotherm representing the majority of cyclization reactions was exhausted halfway through the temperature dwell. Stress and the delta stress values decreased during the final temperature ramp up to @ °C. This happened during the higher temperature ramps (@ °C), and may be a sign that defects were forming.

Looking to the early parts of the temperature profile before the isothermal dwell, the temperatures were increasing in a stepwise fashion. The strain to first failure was quite generous in the first testing point relative to the remainder of the temperature profile. This is because this test was done at @ °C, soon after glass transition of the precursor

fibers (T_g = @ °C). After the glass transition, the polymer is compliant and able to strain to a significant amount. The in-situ stress along the path also shows a significant drop, which is another indicator that the T_g has been passed. The second stress to strain testing point was done at @ °C, just before the onset to the overall rise in stress as a result of the stabilization reactions. Having significantly diminished strain to failure at this point shows that the most compliant region between T_g and T_s is closer to T_g as opposed to closer to the onset of stabilization reactions.

5.3 Thermo-Mechanical Properties During Stabilization

5.3.1 Introduction

Solely observing the amount of strain possible throughout the stabilization process from section 5.2, it can be seen the highest potential for strain exists in a temperature region after the glass transition. Therefore, the next area of study can be to hone in on that temperature region in order to gain a further understanding of stretching in the most compliant region of stabilization. Experiments were performed in order to accurately find the glass transition temperature. Then the thermo-mechanical properties under an array of stresses were tested to see when the fibers were most amenable to stretching. Lastly, a testing array was performed to study if strain rate could produce a trend in allowable strain to fiber breakage.

5.3.2 Method and Equipment

Testing was done on a TA Instruments Q800 series DMA. The sets of experiments were performed on the DDR = 5.9 precursor fibers. Samples were mounted and prepared in the same manner as section 4.2, where epoxy was used to mount the fibers on paper aperture cards.

The first set of experiments was to run the fibers under controlled stress oscillatory testing, where the storage and loss modulus can be studied. The temperature profile selected to study these effects was (Fast) °C/min to (Low) °C, then (Moderate) °C/min for the rest of the test. The tests were selected to end at arbitrary points that were at least as long as the “time to peak stress” values found earlier in this work. The purpose was to clearly identify the glass transition temperature by tan delta peak, and to study the effect

of stress on the storage and loss moduli, in addition to the overall fiber shrinkage. Three tests were run, controlled to (Low) MPa, (Med) MPa, and (High) MPa stress. All other parameters were kept constant, where the testing frequency was 1 Hz, force track 120% (a DMA control parameter), initial preload of 0.01 N, and initial amplitude of 1.0 micron. The tests were carried out under a stress amplitude which in turn, allowed for the fibers to shrink and stretch as needed.

The final batch of experiments that were run were an effort to study the maximum strain that can be imparted to the fibers. Fibers were run in the DMA at (Fast) °C/min up to @ °C. There, stress vs. strain to failure tests were run at an array of three different strain rates, (slow) %/min, (med) %/min, and (fast) %/min. Three specimens at each strain rate were tested.

5.3.3 Results

The stress controlled oscillatory testing of the precursor fiber during stabilization produced storage and loss moduli typical of polymers, showing a glass transition (by tan delta peak) temperature of @ °C after the three runs were averaged. By approximately @ °C, the storage and loss modulus values had plummeted to a fraction of what they once were.

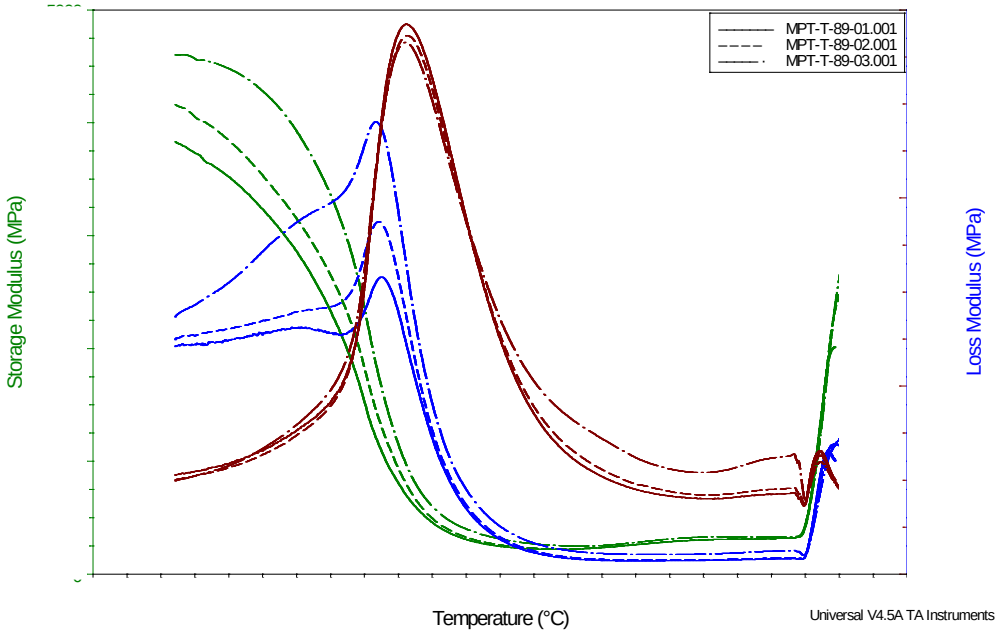

Figure 5-6: Thermomechanical properties of DDR = 5.9 fibers with respect to temperature

When observing the three tests with respect to time, a clearer picture of the mechanical properties after the T_s* of (Low) °C is shown. The selected stress for running the test has a pronounced effect on the properties of the fibers. The higher the stress, the storage modulus values tend to a higher steady state, while taking a longer amount of time to equilibrate.

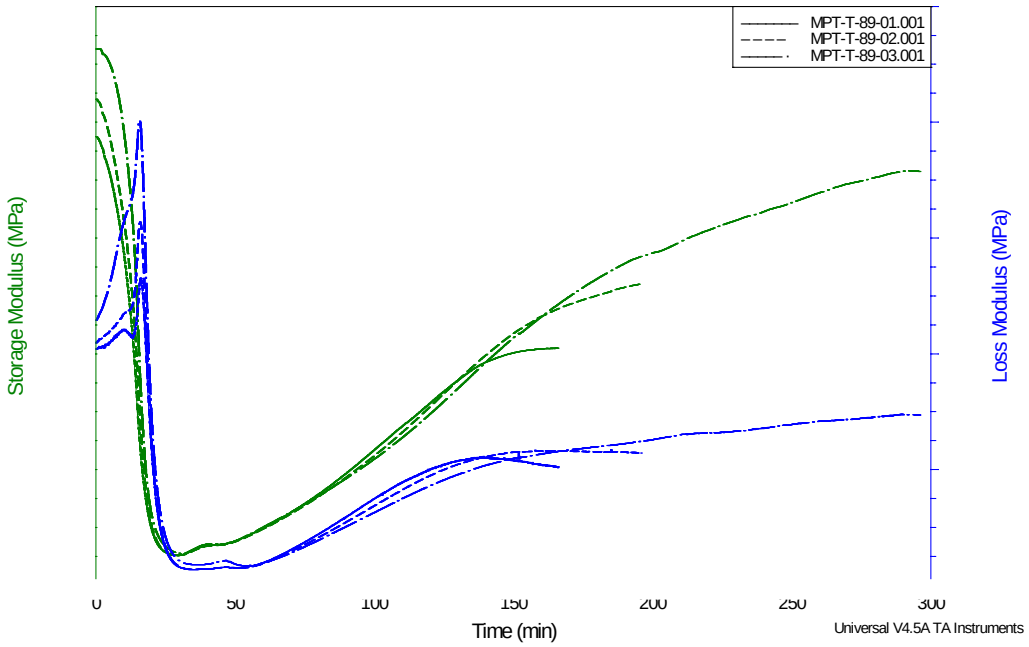

Figure 5-7: ThermoMechanical properties of DDR = 5.9 fibers with respect to time

The imposed stress also had an effect on the resulting displacement of the fibers, whether it was stretching or shrinkage. Tests performed at (Low) and (Med) MPa saw a considerable amount of fiber shrinkage, of @ and @ mm respectively, from the initial gauge length of 10 mm. For the test run at (High) MPa, stretching of nearly @ % occurred after the glass transition temperature, but the shrinkage effects from the chemical reactions of stabilization resulted in the fibers ultimately shrinking by @ mm overall. These trends can be observed in Figure 5-8 below.

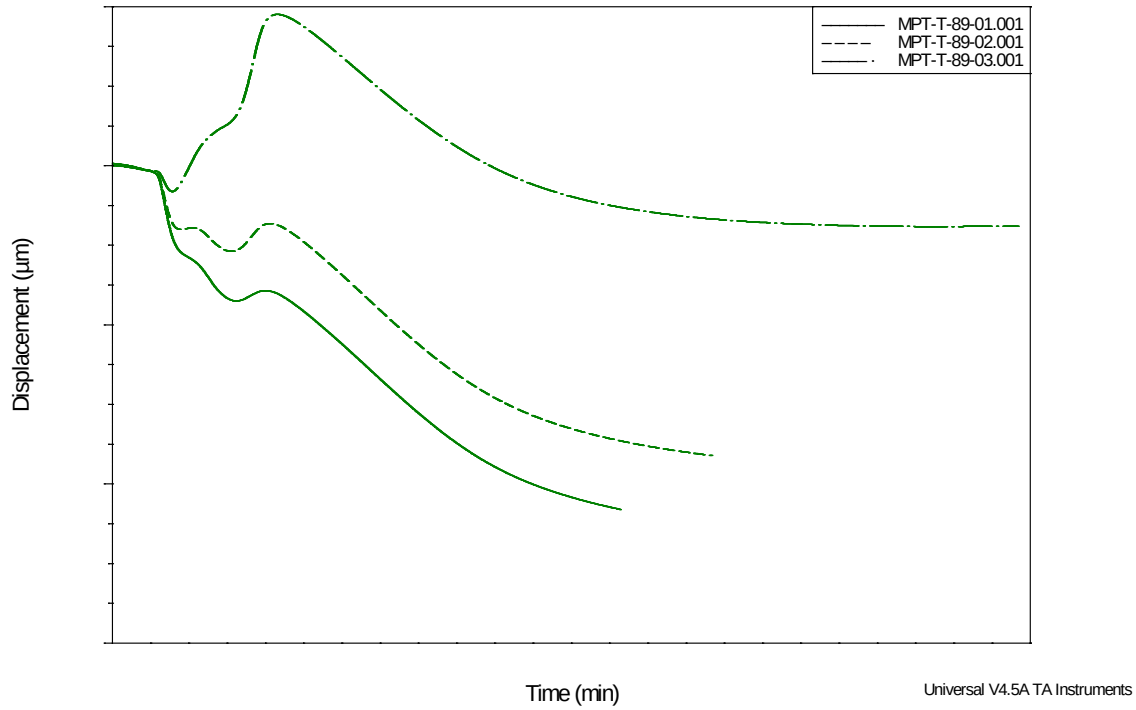

Figure 5-8: Shrinkage behavior of DDR = 5.9 fibers through three stresses

Following the oscillatory experiments to find the thermo-mechanical properties of the precursor fiber, the temperature of @ °C was selected for a series of stress vs. strain tests to failure. The objective was to find the maximum strain that the fibers could withstand, and compare those results to the tests done earlier in section 5.2, where stress vs strain tests were done at @ °C after a stepwise temperature profile.

When observing the stress strain curves, the point where the first sign of fiber breakage occurs is taken to be the breaking point. Since the fibers were held in isostrain conditions leading up to testing temperature, each sample was already under some stress before the test. However, since all conditions were equal leading up the stress vs. strain to failure test, all specimens were at approximately the same stress before the test (@ ± @ MPa). All recorded breaking stresses were taken directly from the results; no subtraction for the

initial stress was performed. Below is a table with the recorded stresses and strains at breakage.

Table 5-3: Results from stress vs. strain tests at an array of strain rates

	Stress at first Break (MPa)			Strain at first Break (%)		
Strain Rate (%/min)	1	5	25	1	5	25
Sample 1						
Sample 2						
Sample 3						
Average						
Std dev						

Comparing between the strain rates of (Low) and (Med) %/min show similar results, within error of each other. Deviating from those two, are the results from the tests done at (High) %/min. The stress at failure is higher, and the corresponding strain is significantly higher.

Comparing those values to those acquired at @ °C in section 5.2, @ %/min resulted in a @ % strain at breakage. This shows that at low strain rates, the contrast between the temperatures of @ °C and @ °C is significant. This further reinforces that the closer to the glass transition temperature, the better for stretching.

5.3.4 Conclusion

The primary objective of the previous set of experiments was to determine the temperature range after the glass transition and before the onset of stabilization reactions. Then once that temperature range was found, find how stress affected the thermo-mechanical properties and also study the effect of strain rate on max allowable strain. It was found that the glass transition temperature (T_g) was @ °C, and when the temperature ramp slowed to (Moderate) °C/min at (Low) °C, the storage and loss modulus values began to rise. This suggests that the activation energy had been reached around that point in the temperature profile. Of note is the relationship between the nominal stress of the tests and the changes seen in the storage and loss moduli, as well as overall length. The higher stress tests resulted in a longer transition time for the modulus values, where the low stress tests that allowed for significant fiber shrinkage saw earlier transition times.

This trend can be explained by the cyclization reactions occurring more easily due to the molecules being allowed to constrict to form the pyridine ring structure.

Secondly, stress vs. strain tests were run at a selected temperature of @ °C. Tests at different strain rates showed a marked increase in allowable strain when the strain was applied at @x higher rate. This can most likely be attributed to the buildup of internal heat from the rapid strain allowing for further stretching. Also, the comparison with earlier tests done at @ °C provided further reinforcement to stretching closer to the glass transition temperature.

5.4 Conclusion

A general study was performed into the stretching of stabilizing fibers. The fibers selected were the same as previous chapters, homopolymer PAN spun at a total draw ratio of 5.9. Stress vs. strain tests throughout the stabilization process were the primary means of study, in order to find the maximum allowable strain, and to look into the mechanical characteristics. During a stabilization procedure that was more conservative than those run in chapter 4, the stabilizing fibers were found to gradually increase in strength and stiffness, whilst decreasing in allowable strain during the chemical reactions of stabilization. Of note, is that halfway through the isothermal dwell for the chemical reactions, the maintained stress while in isostrain conditions flattened out, while stress to failure, strain to failure, and Young's modulus were still changing. A DSC study showed that the stress was increasing during the reaction exotherm period, while flattening when the exotherm ended. This may be indicative to the increase in *in situ* stress being related to the reaction of cyclization. The processes of dehydrogenation and oxidation were seen to continue throughout the temperature treatment, as the Young's modulus was continually increasing long after the reaction exothermic period. Further cross-linking at the final temperature ramp could explain the increased jump in Young's modulus.

Further tests were then directed to the study of thermo-mechanical properties and strain vs. strain rate relationship. Frequency tests found the glass transition to be at @ °C by tan delta peak, and the onset for the increase of storage and loss modulus values was just

at the T_s* value of (Low) °C. The three selected nominal stresses used in testing revealed that the lower the stress, the more shrinkage was observed along with a sooner transition time for the storage modulus. This was attributed to the ease of molecular rearrangement for cyclization when the fibers were allowed to shrink.

Stress versus strain tests were performed at @ °C for three strain rates. When comparing the stress vs strain tests performed here versus the tests done in the first half of this chapter (@ °C), the lower temperature allowed for a higher allowable strain (@ % versus @ % when comparing the similar strain rates). This shows that the selected temperature of @ °C was most likely not the optimal temperature for stretching. Further experimentation with an array of different selected temperatures for the stress vs. strain tests should be explored. With a compliant "range" between @-@ °C, there are many possible levels to observe, but the trend of these data points shows that the closer to the glass transition temperature, the more allowable strain to failure.

6 DESIGN AND COMMISSIONING OF A CONTINUOUS STABILIZATION SYSTEM

All stabilization efforts in this work have been done in a batch process, or held in isostrain conditions, but superior carbon fiber properties are attained through the use of stretching during stabilization. This chapter, modified due to a variety of concerns expressed by the thesis committee, explained the processes that were utilized to create a continuous stabilization furnace with strain control.

To summarize the work that went into this chapter, a number of engineering skills reflective of the author's major (M.S. Mechanical Engineering, Systems and Optimization) were utilized. Engineering design was used to draft, order parts, and construct the machinery used in the stabilization furnace. The priorities of low cost, small use of space, and safety were implemented. Knowledge in experimentation allowed for proper calibration of all moving parts, heating elements, and extraction units. And lastly, systems and optimization skills were needed for the program created to operate the stabilization furnace. One feature of the program was that it was able to use the calibration data and fiber properties found through experimentation to output all parameters needed to successfully stabilize precursor fiber.

7 CONCLUDING REMARKS

Eighteen wt% homopolymer PAN was made into a dope with DMAc and wet-spun with a total draw ratio of 5.9 resulting in fibers with a diameter of 24.15 microns. A portion of that fiber was then hot glycerol stretched to form a precursor fiber with a total draw ratio of 10.7 and an equivalent diameter of 20.60 microns. Both of these precursors were used extensively for this study of stabilization.

The fibers spun at DDR = 5.9 were studied extensively on the DMA for the purposes of studying the relationship between temperature profile and the resulting stress in the fiber when held in isostrain conditions. A simple temperature profile for stabilization was used: an initial heat-up ramp of 5.0 °C/min, a selected T_s* value (temperature selected for reaction initiation), and a h_f temperature ramp for carrying out the reactions of stabilization. A matrix of differing T_s* and h_f values (T_s* = (Low), (Med), (High) °C; h_f = (Slow), (Moderate), (Fast) °C/min) provided an observable trend. It was found that the more conservative the temperature profile (i.e. lower T_s* and h_f), the higher the possible stress during stabilization. However, this came at the cost of time, where the more conservative profiles resulted in a significant increase in time until the peak stress.

The next step was to determine if the peak stress values were any indicator for ultimate carbon fiber tensile properties, and if the time to peak stress values could be a guideline for when the stabilization reactions have completed. Two temperature profiles were selected to be batch stabilized and carbonized with the same parameters as the DMA study to find the final tensile properties. One selected profile resulted in a relatively high stabilization stress, and one with a much lower stress. Those profiles were T_s* = (Low) °C with h_f = (Moderate) °C/min, and T_s* = (High) °C with h_f = (Moderate) °C/min, respectively. Fibers were stabilized under isostrain conditions and removed from heat treatment at the time of peak stress as determined from the DMA experiments. They were then carbonized under identical conditions. Single filament carbon fiber tensile testing showed that the two different temperature profiles provided fibers of very similar characteristics. The higher stress stabilization profile provided a 4.7% increase in

average tensile strength and a 13.3% increase in average tensile modulus, but strength remained entirely within error, while modulus maintained a significant overlap of the error bars. Those two results were then compared to carbon fibers made from identical dope formulations, spinning conditions, and carbonization procedures, but with a much more conservative stabilization profile. It was found that compared to the slow and thorough stabilization procedure, the two shorter procedures maintained a higher tensile strength (still within error) and the modulus for the slower "old" profile was between the two shorter profiles. This led to the conclusion that while saving in stabilization time, a complete stabilization can be achieved using the metric that the stress peak found in DMA studies is an indicator for the completion of stabilization reactions. As far as this study can tell, the maximum values for the *in situ* stress of the stabilizing fibers were not an indicator for better final properties. Further studies with different stabilization profiles and different precursors may prove otherwise. However, the time associated with the peak stress did become a useful parameter in this study.

Studies were also performed on the glycerol stretched fibers, with a combined draw ratio of 10.7 during spinning and subsequent stretching. DSC studies comparing those fibers to the original DDR = 5.9 fibers showed that the glycerol stretched fibers had a higher activation energy. This was most likely attributed to the fibers developing a higher crystalline content and overly stretched amorphous regions (which inhibits the onset of cyclization), or damage to the fibers. The glycerol stretched fibers were also run through several iterations of the DMA temperature profile study, where *in situ* stress was observed in isostrain conditions. The glycerol stretched fibers saw a substantial increase in peak stress values over the DDR = 5.9 fibers. When comparing the two precursor fibers under the same temperature profiles, those higher stresses tended to happen at the same time (within error) as the peak stresses from the original fibers. The slopes of the *in situ* stress were also found to increase at a higher rate and occur slightly later relative to the DDR = 5.9 fibers. The slight delay in the maximum slope for the glycerol stretched fibers reinforces the conclusion raised from the DSC studies. The activation energy has been increased and it could be attributed to changes in the macro-molecular structure of the fibers. The similar time to the peak stress values between the two precursor draw

ratios may indicate that there was marginal difference between the two fibers and the mass and energy diffusion necessary for stabilization reactions. With both precursors in the 20+ micron diameter range, little difference may be seen between them, as opposed to comparing fibers originally spun under different conditions with further reduced precursor diameter.

Additionally, the DDR = 10.7 fibers were batch stabilized under the T_s* = (Low) °C with h_f = (Moderate) °C/min profile, and carbonized under the same conditions as the other fibers. The final carbon fiber tensile properties were found to be significantly diminished. This could only be attributed to the fibers being over-drawn during glycerol stretching to the point of damaging the fibers. This followed the notion that it is possible to stretch precursor fibers too much in the compliant region after the glass transition, as defects were most likely introduced with the aggressive glycerol stretching.

This leads into the experiments done to examine the maximum stretching possible during stabilization. Stress strain tests were performed throughout a conservative temperature profile to study the development of stress and stain at fiber breakage. It was with these experiments that reinforced that stretching during the compliant region between T_g and T_s was the area best suited for the most stretching of stabilizing fibers. Before the glass transition, the fibers are not compliant enough, and the onset of stabilization reactions slowly stiffens the fibers as the linked pyridine rings are formed and strengthens the bonds within the fiber. An array of strain rates were tested, to examine if a trend existed to increase the amount of stretch possible. Increasing the strain rate was found to increase the possible strain by a significant amount. Also, with the selection of temperatures used in the study, it was found that stretching closer to the glass transition temperature yielded more strain versus stretching closer to the reaction onset temperature.

Lastly, the information learned in research and experimentation has led to the modification of a furnace to accommodate PAN based fibers and allow for stretching throughout the stabilization process. Limitations of the furnace were analyzed, including extraction capabilities, to the operating speeds of the furnace. And a program was

created in order to relate the temperature and strain profiles that can be developed through DMA and DSC experimentation, to the furnace equipped with velocity and temperature control.

REFERENCES

1. Morgan, P.E., *Carbon Fibers and Their Composites*. 2005, Boca Raton FL: CRC Press.
2. Fitzer, E., *Pan-Based Carbon-Fibers Present State and Trend of the Technology from the Viewpoint of Possibilities and Limits to Influence and to Control the Fiber Properties by the Process Parameters.* Carbon, 1989. **27**(5): p. 621-645.
3. Savage, G., *Carbon-Carbon Composites*. Vol. 1. 1993, London, England: Chapman & Hall.
4. Donnet, J.B. and R.C. Bansal. Carbon Fibers. Vol. 2nd ed. 1990, New York: Marcel Dekker.
5. Bajaj, P. and A.K. Roopanwal, *Thermal Stabilization of Acrylic Precursors for the Production of Carbon Fibers: An Overview*. Journal of Macromolecular Science, Part C: Polymer Reviews, 1997. **37**(1): p. 97-147.
6. Watt, W., *Production and Properties of High Modulus Carbon Fibres.* Proceedings of the Royal Society of London Series a-Mathematical and Physical Sciences, 1970. **319**(1536): p. 5-&.
7. Gupta, A. and I.R. Harrison, *New aspects in the oxidative stabilization of PAN-based carbon fibers.* Carbon, 1997. **35**(6): p. 809-818.
8. Rennhofer, H., et al., *Structural development of PAN-based carbon fibers studied by in situ X-ray scattering at high temperatures under load.* Carbon, 2010. **48**(4): p. 964-971.
9. Wang, S., et al., *Influence of heat treatment on physical-chemical properties of PAN-based carbon fiber.* Ceramics International, 2006. **32**(3): p. 291-295.
10. Chae, H.G., et al., *Stabilization and carbonization of gel spun polyacrylonitrile/single wall carbon nanotube composite fibers.* Polymer, 2007. **48**(13): p. 3781-3789.
11. Tsai, J.S., *Tension Effects on the Properties of Oxidized Polyacrylonitrile and Carbon-Fibers during Continuous Oxidation.* Polymer Engineering and Science, 1995. **35**(16): p. 1313-1316.
12. Zhang, W.X., J. Liu, and G. Wu, *Evolution of structure and properties of PAN precursors during their conversion to carbon fibers.* Carbon, 2003. **41**(14): p. 2805-2812.
13. Bhat, G.S., et al., *New Aspects in the Stabilization of Acrylic Fibers for Carbon-Fibers.* Carbon, 1990. **28**(2-3): p. 377-385.
14. Bahl, O.P., R.B. Mathur, and K.D. Kundra, *Structure of Pan Fibers and Its Relationship to Resulting Carbon-Fiber Properties.* Fibre Science & Technology, 1981. **15**(2): p. 147-151.
15. Yang, M.C. and D.G. Yu, *Influence of precursor structure on the properties of polyacrylonitrile-based activated carbon hollow fiber*. Journal of Applied Polymer Science, 1996. **59**(11): p. 1725-1731.
16. Mittal, J., R.B. Mathur, and O.P. Bahl, *Post spinning modification of PAN fibres - A review.* Carbon, 1997. **35**(12): p. 1713-1721.
17. Pamula, E. and P.G. Rouxhet, *Bulk and surface chemical functionalities of type IIIPAN-based carbon fibres.* Carbon, 2003. **41**(10): p. 1905-1915.
18. Wiles, K.B., *DETERMINATION OF REACTIVITY RATIOS FOR ACRYLONITRILE/METHYL ACRYLATE RADICAL COPOLYMERIZATION VIA*

NONLINEAR METHODOLOGIES USING REAL TIME FTIR. 2002, Virginia Polytechnic Institute and State University.
19. Traceski, T.F., *Assessing Industrial Capabilities for Carbon Fiber.* Acquisition and Technology, 1999.
20. *Polyacrylonitrile (PAN) Carbon Fibers Industrial Capability Assessment*. 2005, United States Dept. of Defense.
21. Johnson, D.J., *Carbon fibres filaments and composites.* NATO ASI Ser. E, Appl. Sci., 1989. **177**: p. 119.
22. Chung, D.L., *Carbon Fibre Composites*. 1994, Boston: Butterworth-Heinemann.
23. Bahl, O.P. and L.M. Manocha, *Characterization of Oxidized Pan Fibers.* Carbon, 1974. **12**(4): p. 417-423.
24. Bahl, O.P. and R.B. Mathur, *Effect of Load on the Mechanical-Properties of Carbon-Fibers from Pan Precursor.* Fibre Science & Technology, 1979. **12**(1): p. 31-39.
25. Wangxi, Z., L. Jie, and W. Gang, *Evolution of structure and properties of PAN precursors during their conversion to carbon fibers.* Carbon, 2003. **41**(14): p. 2805-2812.
26. Sanchez-Soto, P.J., et al., *Thermal study of the effect of several solvents on polymerization of acrylonitrile and their subsequent pyrolysis.* Journal of Analytical and Applied Pyrolysis, 2001. **58**: p. 155-172.
27. Chung, D.D.L., *Handbook of applied materials science applications-engineering materials in structural electronics, thermal, and other industries.* . 2001, London: CRC Press.
28. Schwartz, M., *Encyclopedia of materials, parts, and finishes.* 2nd ed. 2002, Florida: CRC Press.
29. Rahaman, M., A. Ismail, and A. Mustafa, *A review of heat treatment on polyacrylonitrile fiber.* Polymer Degradation and Stability, 2007. **92**(8): p. 1421-1432.
30. Dalton, S., F. Heatley, and P.M. Budd, *Thermal stabilization of polyacrylonitrile fibres.* Polymer, 1999. **40**(20): p. 5531-5543.
31. Ezekiel, H.M. and R.G. Spain, *Preparation of Graphite Fibers from Polymeric Fibers.* Journal of Polymer Science Part C-Polymer Symposium, 1967(19PC): p. 249-&.
32. Bahl, O.P. and L.M. Manocha, *Shrinkage Behavior of Polyacrylonitrile during Thermal Treatment.* Angewandte Makromolekulare Chemie, 1975. **48**(Nov): p. 145-159.
33. Takaku, A., et al., *Sen-i-Gakkaishi, 38, T-398.* 1982.
34. Grassie, N. and R. McGuchan, *Pyrolysis of polyacrylonitrile and related polymers--III. Thermal analysis of preheated polymers.* European Polymer Journal, 1971. **7**(10): p. 1357-1371.
35. Kakida, H., Polym. Preprints(Japan), Eng. ed., 1992. **41**.
36. Hay, J.N., *Thermal Reactions of Polyacrylonitrile.* Journal of Polymer Science Part a-1-Polymer Chemistry, 1968. **6**(8pa1): p. 2127-&.
37. Minagawa, M., M. Okamoto, and O. Ishizuka, *Specificity of Exothermic Reaction of Polyacrylonitrile.* Journal of Polymer Science Part a-Polymer Chemistry, 1978. **16**(11): p. 3031-3034.

38. Fitzer, E. and D.J. Müller, *The influence of oxygen on the chemical reactions during stabilization of pan as carbon fiber precursor.* Carbon, 1975. **13**(1): p. 63-69.
39. Olive, G.H. and S. Olive, Adv. Polym. Sci., 1983. **51**.
40. Yu, M., et al., *Evolution of tension during the thermal stabilization of polyacrylonitrile fibers under different parameters.* Journal of Applied Polymer Science, 2006. **102**(6): p. 5500-5506.
41. Warner, S.B., L.H. Peebles, and D.R. Uhlmann, *Oxidative stabilization of acrylic fibres.* Journal of Materials Science, 1979. **14**(3): p. 556-564.
42. Bai, Y.-J., et al., *HRTEM microstructures of PAN precursor fibers.* Carbon, 2006. **44**(9): p. 1773-1778.
43. Wu, G., et al., *Influence of tension on the oxidative stabilization process of polyacrylonitrile fibers.* Journal of Applied Polymer Science, 2005. **96**(4): p. 1029-1034.
44. Lian, F., et al., *Stretching-induced deformation of polyacrylonitrile chains both in quasicrystals and in amorphous regions during the in-situ thermal modification of fibers prior to oxidative stabilization.* Carbon, (0).
45. Masson, J.C., *Acrylic Fiber Technology and Applications*. 1995.
46. Ltd., T.C. 1985: Japan.
47. Bajaj, P. and M. Padmanaban, *Thermal-Behavior of Copolymers of Acrylonitrile with Haloalkyl Acrylates or Methacrylates.* European Polymer Journal, 1985. **21**(1): p. 93-96.
48. Coleman, M.M. and G.T. Sivy, *Fourier-Transform Ir Studies of the Degradation of Polyacrylonitrile Co-Polymers .1. Introduction and Comparative Rates of the Degradation of 3 Co-Polymers Below 200-Degrees-C and under Reduced Pressure.* Carbon, 1981. **19**(2): p. 123-126.
49. Moreton, R. and W. Watt, *The spinning of polyacrylonitrile fibres in clean room conditions for the production of carbon fibres.* Carbon, 1974. **12**(5): p. 543-554.
50. Mathur, R.B., et al., *Modification of Pan Precursor - Its Influence on the Reaction-Kinetics.* Carbon, 1988. **26**(3): p. 295-301.
51. Damodaran, S., P. Desai, and A.S. Abhiraman, *Chemical and Physical Aspects of the Formation of Carbon Fibres from PAN-based Precursors.* Journal of the Textile Institute, 1990. **81**(4): p. 384 - 420.
52. Riggs, D.M., R.J. Shuford, and R.W. Lewis, *Handbook of composites*. 1987, New York: Van Nostrand Reinhold.
53. Donnet, J.B., et al., *Carbon fiber*. 3rd ed. 1998.
54. Fitzer, E., W. Frohs, and M. Heine, *Optimization of stabilization and carbonization treatment of PAN fibres and structrual characterization of the resulting carbon fibres.* Carbon, 1985. **24**(4): p. 8.
55. Liu, Y., H.G. Chae, and S. Kumar, *Stabilization of Gel-Spun Polyacrylonitrile/Carbon Nanotubes Composite Fibers. Part II: Stabilization Kinetics and Effects of Various Chemical Reactions.*, in *School of Polymer, Textile and Fiber Engineering*. 2010, Georgia Institute of Technology: Atlanta. p. 23.
56. Bansal, R.C., J.B. Donnet, and F. Stoeckli, *Active Carbon*. 1988, New York: Marcel Dekker Inc.

57. Houtz, R.C., *"Orlon" Acrylic Fiber: Chemistry and Properties.* Textile Research Journal, 1950. **20**: p. 16.
58. Friedlander, H.N., et al., *On the Chromophore of Polyacrylonitrile. VI. Mechanism of Color Formation in Polyacrylonitrile.* Macromolecules, 1968. **1**(1): p. 79-86.
59. Burlant, W.J. and J.L. Parsons, *Pyrolysis of polyacrylonitrile.* Journal of Polymer Science, 1956. **22**(101): p. 249-256.
60. Grassie, N. and R. McGuchan, *Pyrolysis of polyacrylonitrile and related polymers--I. Thermal analysis of polyacrylonitrile.* European Polymer Journal, 1970. **6**(9): p. 1277-1291.
61. Thompson, E.V., *The thermal behavior of acrylonitrile polymers. I. On the decomposition of polyacrylonitrile between 250 and 325°C.* Journal of Polymer Science Part B: Polymer Letters, 1966. **4**(5): p. 361-366.
62. Grassie, N. and R. McGuchan, *Pyrolysis of polyacrylonitrile and related polymers--VI. Acrylonitrile copolymers containing carboxylic acid and amide structures.* European Polymer Journal, 1972. **8**(2): p. 257-269.
63. Schurz, J., *Discoloration effects in acrylonitrile polymers.* Journal of Polymer Science, 1958. **28**(117): p. 438-439.
64. Peebles, L.H., et al., *Basic dyeability and acid content of high-conversion polyacrylonitrile.* Journal of Applied Polymer Science, 1972. **16**(12): p. 3341-3351.
65. Peebles Jr, L.H., et al., *On the exotherm of polyacrylonitrile: Pyrolysis of the homopolymer under inert conditions.* Carbon, 1990. **28**(5): p. 707-715.
66. Liu, Y., et al., *Stabilization of Gel-Spun Polyacrylonitrile/Carbon Nanotubes Composite Fibers. Part III: Effects of Stabilization Conditions.*, in *School of Polymer, Textile and Fiber Engineering*. 2010, Georgia Institute of Technology: Atlanta. p. 23.
67. Yun, J.-H., et al., *Process Optimization for Preparing High Performance PAN based Carbon Fibers.* Bull. Korean Chem. Soc., 2009. **30**(10): p. 6.
68. Kissinger, H.E., *Reaction Kinetics in Differential Thermal Analysis.* Analytical Chemistry, 1957. **29**(11): p. 1702-1706.
69. Sen, K., P. Bajaj, and T.V. Sreekumar, *Thermal Behavior of Drawn Acrylic Fibers.* Journal of Polymer Science Part B: Polymer Physics, 2003. **41**(22).
70. Liu, J., et al., *Thermo-chemical reactions occurring during the oxidative stabilization of electrospun polyacrylonitrile precursor nanofibers and the resulting structural conversions.* Carbon, 2009. **47**(4): p. 1087-1095.
71. Bashir, Z., *A critical review of the stabilization of polyacrylonitrile.* Carbon, 1991. **29**(8): p. 9.
72. Cai, J., et al., *Effect of strain rate on the compressive mechanical of aluminum alloy matrix composite filled with discontinuous carbon fibers properties.* Materials Science and Engineering a-Structural Materials Properties Microstructure and Processing, 2008. **485**(1-2): p. 681-689.
73. Ozawa, T., *A New Method of Analyzing Thermogravimetric Data.* Bulletin of the Chemical Society of Japan, 1965. **38**(11): p. 1881-&.

VITA

Mark Parr Taylor, EIT

Born: 13 July 1986 – Harrisburg, Pennsylvania

Education:

- Bachelors of Science Mechanical Engineering
  - University of Kentucky
  - Degree Earned: May 2010 (Magna Cum Laude, with Honors)
- High School Diploma
  - Northern High School
  - Class of 2005

Positions Held:

- Graduate Research Assistant
  - University of Kentucky Center for Applied Energy Research
- Undergraduate Research Assistant
  - University of Kentucky Center for Applied Energy Research
- Co-op Intern
  - Lexmark International, Inc. (Lexington, KY)
- Team Race Manager
  - University of Kentucky Solar Car Team
- President
  - Pi Lambda Chapter of Pi Tau Sigma

Honors

- Member of Tau Beta Pi, Kentucky-Alpha Chapter (Engineering Honor Society)
- Member of Pi Tau Sigma, Pi Lambda Chapter (Mechanical Engineering Honor Society)
- “Best in Show, Manager’s Choice” for poster presentation at Lexmark’s First Annual Student Symposium